DEVELOPMENT OF A COMPUTER AIDED ENGINEERING TOOL FOR
PIPE LINES

A THESIS SUBMITTED TO
THE GRADUATE SCHOOL OF NATURAL AND APPLIED SCIENCES
OF
MIDDLE EAST TECHNICAL UNIVERSITY

KEMAL YÜCE AYDINOĞLU

IN PARTIAL FULFILLMENT OF THE REQUIREMENTS
FOR
THE DEGREE OF MASTER OF SCIENCE
IN
CIVIL ENGINEERING

OCTOBER 2016

Approval of the thesis:

DEVELOPMENT OF A COMPUTER AIDED ENGINEERING TOOL FOR PIPE LINES

submitted by **KEMAL YÜCE AYDINOĞLU** in partial fulfillment of the requirements for the degree of **Master of Science in Civil Engineering Department, Middle East Technical University** by,

Prof. Dr. Gülbin Dural ÜNVER
Dean, Graduate School of **Natural and Applied Sciences**   _____

Prof. Dr. İsmail Özgür YAMAN
Head of Department, **Civil Engineering**   _____

Prof. Dr. Zafer BOZKUŞ
Supervisor, **Civil Engineering Department, METU**   _____

Dr. Erdal OKTAY
Co-supervisor, **EDA Ltd. Co., ODTÜ Teknokent**   _____

Examining Committee Members:

Prof. Dr. İsmail AYDIN
Civil Engineering Department, METU   _____

Prof. Dr. Zafer BOZKUŞ
Civil Engineering Department, METU   _____

Prof. Dr. Hasan U. AKAY
Mechanical Engineering Department, ATILIM UNIVERSITY _____

Assoc. Prof. Dr. Nuri MERZİ
Civil Engineering Department, METU   _____

Assoc. Prof. Dr. Mete KÖKEN
Civil Engineering Department, METU   _____

Date: _____

I hereby declare that all information in this document has been obtained and presented in accordance with academic rules and ethical conduct. I also declare that, as required by these rules and conduct, I have fully cited and referenced all material and results that are not original to this work.

Name, Last Name: KEMAL YÜCE AYDINOĞLU

Signature   :

ABSTRACT

DEVELOPMENT OF A COMPUTER AIDED ENGINEERING TOOL FOR PIPE LINES

Aydınoğlu, Kemal Yüce

M.S., Department of Civil Engineering

Supervisor   : Prof. Dr. Zafer BOZKUŞ

Co-Supervisor   : Dr. Erdal OKTAY

OCTOBER 2016, 113 pages

A computer program is developed to solve pipe network problems for incompressible fluids. It is intended to run under the Computer Aided Engineering software package $CAEeda^{TM}$. The finite element method is employed to model the governing equations. The accuracy of the program is validated by comparing the results of five test case problems choosen from a reference literature. The good agreement between present program and reference solutions is observed. By using geometry, pre-process and post-process capabilities of $CAEeda^{TM}$, as a result of the program integration, complex pipe network systems can be analyzed easily. Consequently, it may be used as a promising tool for pipe network analysis.

Keywords: Pipe Network, Pipe Flow, Finite Element Method, Computer Aided Engineering

ÖZ

BORU HATLARI İÇİN BİLGİSAYAR DESTEKLİ BİR MÜHENDİSLİK
ARACININ GELİŞTİRİLMESİ

Aydınoğlu, Kemal Yüce

Yüksek Lisans, İnşaat Mühendisliği Bölümü

Tez Yöneticisi : Prof. Dr. Zafer BOZKUŞ

Ortak Tez Yöneticisi : Dr. Erdal OKTAY

Ekim 2016 , 113 sayfa

Sıkıştırılamaz akışkanlar için boru şebekesi problemlerini çözen bir bilgisayar programı geliştirilmiştir. Bilgisayar destekli mühendislik yazılım paketi $CAEeda^{TM}$ altında çalışması amaçlanmıştır. Denklemleri çözmek için sonlu elemanlar yöntemi uygulanmıştır. Programın dogruluğu; referans literatüründen seçilen beş test problemle kıyaslanarak teyit edilmiştir. Mevcut program ile referans çözümler arasında iyi uyum olduğu gözlenmiştir. Programın entegrasonu sonucu $CAEeda^{TM}$'nın geometri, önişlemci ve sonişlemci yetenekleri kullanılarak kompleks boru şebekeleri kolaylıkla analiz edilebilmektedir. Bu sayede program boru şebeke analizleri için gelecek vaat eden bir araç olarak kullanılabilir.

Anahtar Kelimeler: Boru Şebekesi, Borularda Akış, Sonlu Elemanlar Yöntemi, Bilgisayar Destekli Mühendislik

vi

To my family

Zahide Belma Işıkcı, Neriman Tuğçe Aydınoğlu

ACKNOWLEDGMENTS

TABLE OF CONTENTS

APPENDICES

LIST OF TABLES

TABLES

LIST OF FIGURES

FIGURES

xvi

LIST OF SYMBOLS AND NOMENCLATURE

L	Pipe Length
X	Global Coordinate X
Y	Global Coordinate Y
Z	Global Coordinate Z or Elevation Head
X_i	Global Coordinate X at the ith node
Y_i	Global Coordinate Y at the ith node
Z_i	Global Coordinate Z at the ith node
X_j	Global Coordinate X at the jth node
Y_j	Global Coordinate Y at the jth node
Z_j	Global Coordinate Z at the jth node
D	Pipe Diameter
C_{HW}	Hazen-William's Roughness Coefficient
n	Manning's Roughness Coefficient
f	Darcy-Weisbach Friction Factor
γ	Specific Weight
g	Earth's Standard Gravity
H	Total Head
H_i	Total Head at the ith node
H_j	Total Head at the jth node
P	Pressure
P_i	Pressure at the ith node
P_j	Pressure at the jth node
P/γ	Pressure Head
P/γ_i	Pressure Head at the ith node
P/γ_j	Pressure Head at the jth node
V	Fluid Velocity
V_i	Fluid Velocity at the ith node
V_j	Fluid Velocity at the jth node

$V^2/2g$	Kinetic Energy Head
$V_i^2/2g$	Kinetic Energy Head at the ith node
$V_j^2/2g$	Kinetic Energy Head at the jth node
M	Number of Source Nodes
N	Number of Demand Nodes
C	Number of Loops
k_{ij}	Resistance Constant in an element Connected to Node i and j
Q_{ij}	Discharge in an element Connected to Node i and j
Q_i	Demand Discharge at the ith node
Q_j	Demand Discharge at the jth node
q_j	Demand Discharge at the jth node
h_l	Head Loss
h_{ij}	Head Loss at an element Connected to Node i and j
$h_{l(pipe)}$	Head Loss of Pipe Element
$h_{l(fitting)}$	Head Loss of Pipe Element
$h_{l(pump)}$	Head Loss of Pump Element
ε	Roughness Height of the Pipe Wall
Re	Reynold's Number
ν	Kinematic Viscosity
K_{pipe}	Hazen-William Constant
$K_{fitting}$	Fitting Loss Coefficient
COH	Cut of Head
A	Cross-sectional Area
A_i	Cross-sectional Area at the ith node
A_j	Cross-sectional Area at the jth node
CAD	Computer Aided Design
CFD	Computational Fluid Dynamics
CSD	Computational Solid Dynamics
GUI	Graphical User Interface

CHAPTER 1

INTRODUCTION

In the present study, it is intended to develop a computer aided design tool for mainly water distribution lines and networks, etc. by using the finite element method. The objective is to append the developed software to EDA Engineering's multidisciplinary general purpose software, named $CAEeda^{TM}$ [1]. $CAEeda^{TM}$ has powerful built-in CAD, pro- and post-process, or modules as well as CFD, CSD analysis and design optimization modules. As a result, the pipe flow program developed here can be used as a part of $CAEeda^{TM}$ for large systems.

Water distribution systems are important components of civil engineering works as they continuously supply required amount of precious water for domestic, commercial, public and industrial purposes. In domestic use, water is required for drinking, cooking, and washing including, heating and cooling, air conditioning, sanitary purposes, etc. Examples of other uses can be a long list which is beyond the scope of the study.

An efficient water supply system includes various facilities for accumulating and storing water such as dam reservoirs or large tanks, pipelines for transportation, if necessary, pumping and treatment plants, etc. In general, water is conveyed through a main line from a reservoir to a treatment plant where water is treated to get it ready for the consumption of the people. After treatment, it would be distributed to pipe networks from which the end users would receive the water. Thus, it is an important task of the civil engineers or water supply engineers to evaluate accurately the demands of water and supply amount of the water and the means to convey it properly to the users. Typically, water distribution

networks are made up of pipelines, pipe elements such as elbows, tee sections, valves, pumps, etc. It is the job of the engineers to provide proper number of them in a given network to achieve the goals. Discharge in each pipe should be calculated and also the demands wherever they exist should be satisfied. It is also important that the pipe network system is always under a reasonable pressure head to maintain the safe operation. To achieve all these, an engineer must perform many analyses, by using and changing various parameters such as pipe material, pipe diameter, pipe lengths, location of the valves, pumps, etc. One can realize that this is very complicated, time-consuming and repetitious work that require the aid of computers.

Consequently, some numerical methods have been developed to do the task of analyzing pipe networks for which commercial software such as WaterCAD-Bentley [2], AFT Piping Software [3] and open source software EPANET [4] are available. Also, Mohtar et al. [5] developed a finite element program named ANALYZER in 1991. The purpose of this thesis is to develop a finite element program for steady, incompressible flows through general piping systems, $CAEeda^{TM}$ to be used for pipe network optimizations.

Most common numerical methods for analyzing pipe networks are Hardy-Cross Method, Newton-Raphson Method, Linear Theory Method and Finite Element Method. They will all be introduced briefly in the thesis. However, it is one of the goals of this study to use the Finite Element Method to analyze the water distribution networks.

Finite element methods and techniques have already been well established. In the finite element method, a given physical problem is modeled by dividing it into some small parts called "elements". This is followed by an analysis of the physics of the problem performed on these elements. Ultimately, the elements are put together to present the whole picture that is the solution to the original problem.

CHAPTER 2

WATER DISTRIBUTION NETWORKS

2.1 Definitions

Pipe Networks may be divided into three types, serial, branching, and looped networks. They are defined as follows.

2.1.1 Types of Networks

2.1.1.1 Serial Network

Serial Network is a network which has no branches or any loops. It is a configuration in which pipe segments are connected in series form. It is shown in Figure 2.1. It is the simplest network among all types of networks.
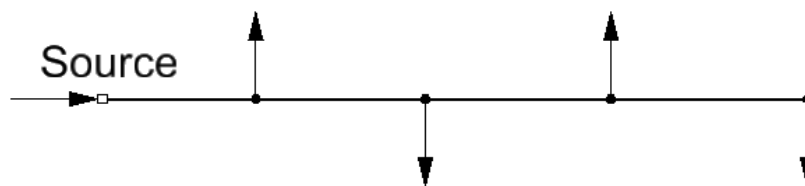
Figure 2.1: Serial Network [6]

2.1.1.2 Branching Network

It is also called dead-end network. Branching Network is a network which has branches but no loops. In other words, it consists of serial networks and these networks do not include any loops, Figure 2.2.
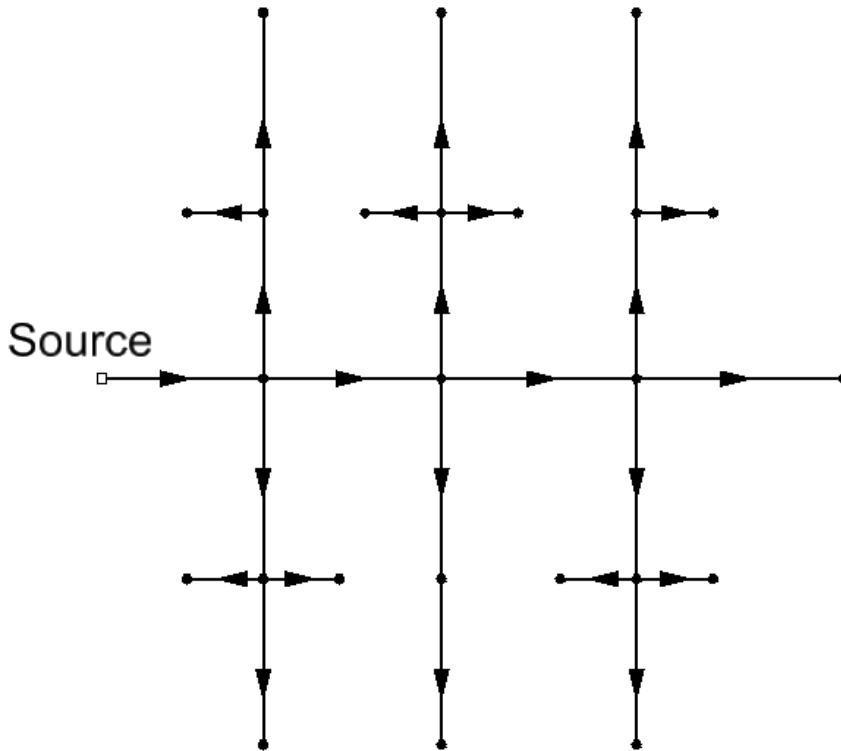
Figure 2.2: Branching Network [6]

2.1.1.3 Looped Network

Looped network is a network which consists of loops. It may contain also branches or serial parts. However, it should have at least one loop to be considered looped network shown in Figure 2.3. Bhave [6] stated that serial and branching networks are not appropriate for repairs or replacements because there is only one path for fluid flow. However, in the looped network, a part of the system can be closed to fix or replace some of the parts in loop while fluid continues to flow. He also expressed looped network is more reliable than the other two network types due to existence of alternative paths. On the other hand,

4

looped networks are more expensive compared to serial and branching network.
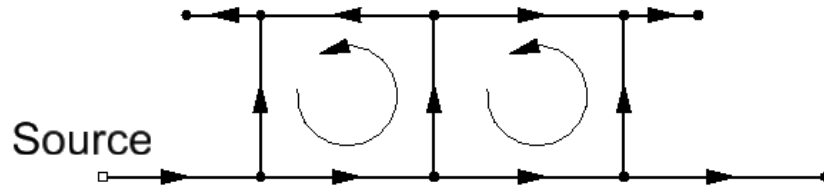
Figure 2.3: Looped Network [6]

2.1.2 Pipe Parameters

A pipe network can be constructed with pipes, pumps, and fittings which may be a bend, tee, contraction, expansion, and valves. Before analyzing a pipe network, some important parameters should be defined. It is done in the next sections.

2.1.2.1 Pipe Length

Pipe length, whose SI unit is meter, is a parameter of pipe which can be calculated from the known geography. It is obtained by the Cartesian node coordinates, X, Y, and Z. When the node coordinates are known, the pipe length can be easily calculated with the equation below.

$$L = \sqrt{(X_i - X_j)^2 + (Y_i - Y_j)^2 + (Z_i - Z_j)^2} \qquad (2.1)$$

Where i represents the ith node of the pipe element, j represents the jth node of the pipe element, L represents length of the pipe element.

2.1.2.2 Pipe Diameter

Pipe diameter (D) is in meters and it is a known parameter while analyzing the pipe network.

2.1.2.3 Pipe Roughness Coefficient

This is a unitless parameter. There are two types of head loss formula, and each one has a different pipe roughness coefficient. These are namely Hazen-William coefficient (C_{HW}) and Darcy-Weisbach friction factor (f). Darcy-Weisbach friction factor is also dependent on pipe discharge in addition to roughness of the pipe material. Thus, it is changing while analyzing the pipe network. On the other hand, Hazen-William coefficient is constant during the pipe network analysis because it is independent of pipe discharge.

2.1.2.4 Minor Head Loss Coefficient

Minor head loss coefficient is a unitless coefficient which is changing for different network elements. These elements can be bend, tee, valve, contraction, or expansion of pipe.

2.1.2.5 Demand Pattern

Demand pattern is a nodal parameter. It generally fluctuates with time. However, in pipe network analysis, steady-state conditions are considered.

2.1.2.6 Source Supply Pattern

Source supply pattern is also a nodal parameter. It is dependent on the nodal demands at the steady-state condition. For example, reservoirs are thought to be source supply pattern.

2.1.2.7 Energy Grade Line Level at Demand Nodes

Energy grade line level is the sum of pressure head (P/γ), the elevation head (Z) , and kinetic energy head ($v^2/2g$) . This parameter, called H in Equation 2.2 is generally unknown at the demand nodes. However, demand discharge is

known at these nodes. In addition to these, kinetic energy head term is normally neglected in the network calculations because its value is too small compared to other terms.

$$H = \frac{P}{\gamma} + Z + \frac{V^2}{2g} = Total\ Head \tag{2.2}$$

2.1.2.8   Energy Grade Line Level at Source Nodes

This parameter (H) is usually known parameter at the source nodes and it is constant during the steady-flow analysis, such as reservoir water level.

2.1.3   Parameter Interrelationships

Basic energy equation from i^{th} node of the element to j^{th} node of the element is written as follows.

$$\frac{P_i}{\gamma} + Z_i + \frac{V_i^2}{2g} = \frac{P_j}{\gamma} + Z_j + \frac{V_j^2}{2g} + h_l \tag{2.3}$$

where h_l is the head loss term.

Energy Equation for pipe networks is a nonlinear equation, because of the head loss term. Since there is no direct solution for a nonlinear equation, numerical solution (iterative solution) methods are used to solve these kinds of problems. In this chapter, the types of iterative solution methods for the pipe networks in steady-flow analysis will be explained. Before explaining the solution methods, some parameters which interrelates these solution types will be covered.

Consider a looped network which has M source nodes, N demand nodes, X pipes, and C loops that are shown in Figure 2.4.
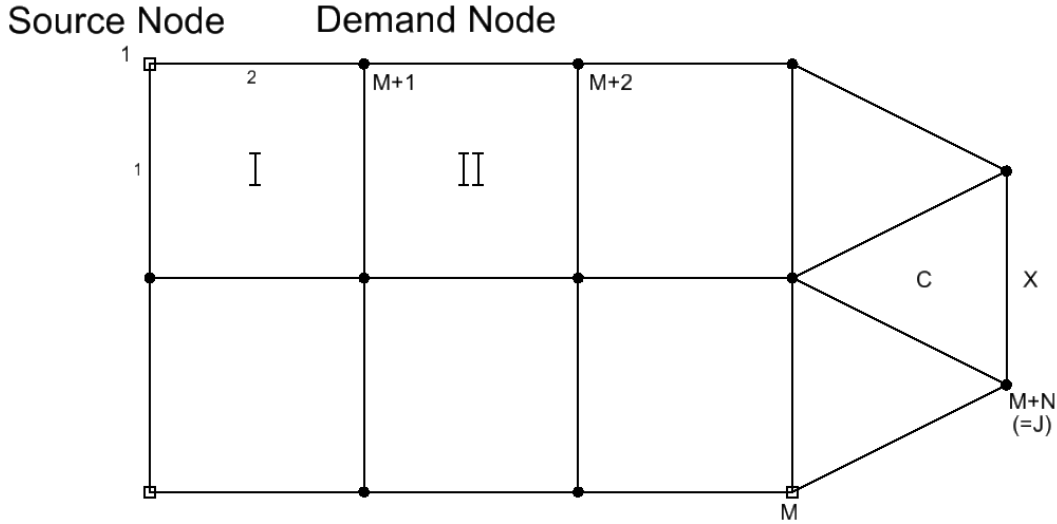
Figure 2.4: Detailed Looped Network [6]

The relationship between these values is shown in Equation 2.4.

$$X = M + N + C - 1 \tag{2.4}$$

Where X illustrates the number of pipes. X may be represented as ij.

For the network analysis, there are three types of relationships, which will be covered next.

2.1.3.1 Pipe Head Loss Relationship

In a pipe segment of ij, from the energy equation, the general head loss formula is obtained as follows.

$$h_{ij} = k_{ij}Q_{ij}^n = H_i - H_j \tag{2.5}$$

where the terms h_{ij}, k_{ij}, Q_{ij}, H_i, H_j, n represent the head loss in pipe ij, the resistance constant which can change by the Hazen-William (HW), Darcy-Weisbach (DW), or Manning equation, pipe discharge, hydraulic grade line elevation at i^{th} and j^{th} node of the element, and discharge exponent, respectively. While analyzing the network, the flow direction may reverse. When the flow direction reverses, the discharge sign will change and become negative. To ccount for the change in flow direction, Equation 2.5 will be rewritten as follows.

8

$$h_{ij} = H_i - H_j = k_{ij}|Q_{ij}|^{n-1}Q_{ij} \qquad (2.6)$$

When hydraulic grade line level at the ith node is greater than the one at the jth node ($H_i > H_j$), Q_{ij} will be positive. Otherwise, Q_{ij} will be negative. Equation 2.6 is sometimes expressed as

$$h_{ij} = k'_{ij}Q_{ij} \qquad (2.7)$$

Where $k'_{ij} = k_{ij}|Q_{ij}|^{n-1}$

This form is called the linearized form according to Bhave [6]. Equation 2.5 can also be written as follows.

$$Q_{ij} = \left(\frac{H_i - H_j}{k_{ij}}\right)^{1/n} \qquad (2.8)$$

To account for the change in the flow direction, Equation 2.8 can be rewritten as follows.

$$Q_{ij} = \left(\frac{H_i - H_j}{k_{ij}^{1/n}|H_i - H_j|^{\left(1-\frac{1}{n}\right)}}\right)^{1/n} \qquad (2.9)$$

Whose sign is positive while flow direction is from i to j.

Equation 2.9 can also be expressed as follows.

$$Q_{ij} = C'_{ij}(H_i - H_j) \qquad (2.10)$$

where $C'_{ij} = \frac{1}{k_{ij}^{1/n}|H_i-H_j|^{\left(1-\frac{1}{n}\right)}}$ in which C'_{ij} is called modified conductance of pipe.

2.1.3.2 Node Flow Continuity Relationship

In a steady-state, incompressible flow in a pipe network, the continuity equation must be satisfied at a node. In other words, inflow must be equal to the outflow. Therefore,

$$\sum_{\substack{pipe\ connected \\ to\ j}} Q_{ij} + q_j = 0 \qquad (2.11)$$

9

Where q_j is external flow, either supply(inflow) or demand (outflow) at node j, and Q_{ij} is the discharge in the pipe.

The equation above gives $(M + N)$ times linear relationships in terms of the pipe discharge. This equation can also be written as follows.

$$\sum_{\substack{i \text{ connected to} \\ j \text{ through pipe}}} \left(\frac{H_i - H_j}{k_{ij}} \right)^{\frac{1}{n}} + q_j = 0 \tag{2.12}$$

When we rewrite the equations, it is formed below.

$$\sum_{\substack{i \text{ connected to} \\ j \text{ through pipe}}} \left(\frac{H_i - H_j}{k_{ij}^{1/n} |H_i - H_j|^{\left(1 - \frac{1}{n}\right)}} \right) + q_j = 0 \tag{2.13}$$

When this equation includes hydraulic grade line values, it becomes nonlinear equation. If we try to linearize this equation which contains hydraulic grade line values, it will be as follows.

$$\sum_{\substack{i \text{ connected to} \\ j \text{ through pipe}}} C_x' (H_i - H_j) + q_j = 0 \tag{2.14}$$

Where $C_x' = \dfrac{1}{k_{ij}^{1/n} |H_i - H_j|^{\left(1 - \frac{1}{n}\right)}}$

2.1.3.3   Loop Head Loss Relationship

For all loops of a pipe network, summation of all the head losses in the pipes forming a loop must be zero. It is shown in Equation 2.15.

$$\sum_{\substack{pipe \in loop}} h_{ij} = \sum_{\substack{pipe \in loop}} k_{ij} Q_{ij}^n = 0 \tag{2.15}$$

If this equation is linearized, it can take the following form.

$$\sum_{\substack{pipe \in loop}} h_{ij} = \sum_{\substack{pipe \in loop}} k_{ij}' Q_{ij} = 0 \tag{2.16}$$

Where $k_{ij}' = k_{ij} |Q_{ij}|^{n-1}$

10

2.1.4 Solution Methods

As mentioned previously, energy equation for pipe networks is a nonlinear equation because of the head loss term. Since there is no direct solution for nonlinear equations, numerical solutions, also called iterative solutions, are used to solve these equations. In this chapter, the types of iterative solution methods will be explained for pipe networks in a steady flow.

2.1.4.1 Hardy Cross Method

According to Bhave [6], Hardy Cross [7] might be the first person who suggested in 1936 an iterative solution for network analyses. His approach is based on ΔQ equations which are loop flow correction equations. This approach is called method of balancing heads. After that Cornish [8] also applied the same procedure to nodal head correction equations which are ΔH equations. This approach is also called method of balancing flows. Both ΔQ equations and ΔH equations belong to the Hardy Cross Method.

It has the following assumptions.

1. At a given time, only one equation is solved from the available set of ΔQ equations.

2. There is only one ΔQ equation for each loop. The effect of adjacent loops is ignored.

3. Each term of modified ΔQ equation is expanded in a Taylor's series and higher-powers of ΔQ terms are neglected except the first-power ΔQ terms.

Let us consider a single loop of a network in Figure 2.5. There are four pipes and they are labeled as a, b, c, and d. The known resistance constant k with a proper

subscript for each pipe is indicated in the figure as k_a, k_b, k_c and, k_d, respectively. Also assumed discharges are shown accordingly for each pipe satisfying the node-flow continuity relationships. The ΔQ equation can be written for the loop of Figure 2.5 as shown below.
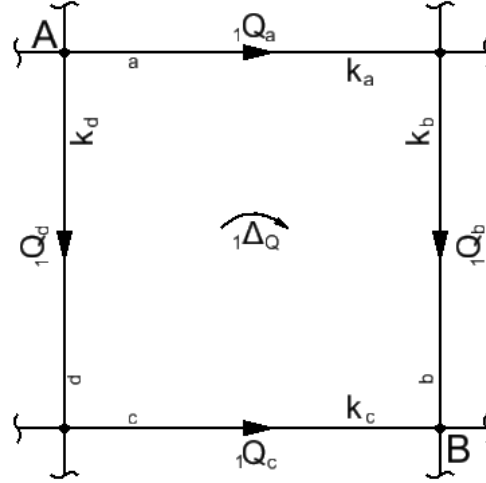
Figure 2.5: Single Loop of distribution network [6]

$$k_a({}_1Q_a +_1 \Delta Q)^n + k_b({}_1Q_b +_1 \Delta Q)^n$$
$$- k_c({}_1Q_c -_1 \Delta Q)^n - k_d({}_1Q_d -_1 \Delta Q)^n = 0 \quad (2.17)$$

When we expand this equation in a Taylor's series and ignore the higher power of ΔQ terms, it will become:

$$k_a({}_1Q_a^n + n \cdot_1 Q_a^{n-1} \cdot_1 \Delta Q) + k_b({}_1Q_b^n + n \cdot_1 k_b^{n-1} \cdot_1 \Delta Q)$$
$$- k_c({}_1Q_c{}^n - n \cdot_1 Q_c^{n-1} \cdot_1 \Delta Q) - k_d({}_1Q_d^n - n \cdot_1 Q_d^{n-1} \cdot_1 \Delta Q) = 0 \quad (2.18)$$

If we rearrange this equation for ${}_1\Delta Q$, we get

$$_1\Delta Q = -\frac{k_a \cdot_1 Q_a^n + k_b \cdot_1 Q_b^n - k_c \cdot_1 Q_c^n - k_d \cdot_1 Q_d^n}{k_a \cdot n \cdot_1 Q_a^{n-1} + k_b \cdot n \cdot_1 Q_b^{n-1} + k_c \cdot n \cdot_1 Q_c^{n-1} + k_d \cdot n \cdot_1 Q_d^{n-1}} \quad (2.19)$$

Further, it can be written as

$$_1\Delta Q = -\frac{\sum k_i \cdot_1 Q_i^n}{\sum |n \cdot k_i \cdot_1 Q_i^{n-1}|} \quad (2.20)$$

12

If this equation is generalized for all loops,

$$_t\Delta Q = -\frac{\sum\limits_{i\in loop} k_i \cdot_t Q_i^n}{\sum\limits_{i\in loop} |n \cdot k_i \cdot_t Q_i^{n-1}|} \tag{2.21}$$

Where t is the number of iteration steps. Consequently, a ΔQ equation developed for each loop, will be solved simultaneously for the entire network to compute the discharge in each pipe.

2.1.4.2 Newton-Raphson Method

Newton-Raphson Method may be considered as improved version of Hardy Cross Method. Bhave [6] stated that in Hardy Cross Method, the effect of ignoring the adjacent loops and considering about only one correction equation at a time is considerable. Apart from this, while increasing the size of a network, number of iteration steps is rising. Thus, if all the adjacent loops are considered to be solved simultaneously, while achieving the solution in Newton-Raphson method, the numbers of iteration steps are considerably less than that of Hardy-Cross method. Again, since the energy equation is nonlinear due to head loss term in general, iterative procedure is necessary for its solution. The general expression for the Taylor's series is as follows.

$$F(a+b) = F(a) + bF'(a) + \frac{b^2}{2!}F''(a) + ... + \frac{b^{n-1}}{(n-1)!}F^{n-1}(a)$$
$$+ \frac{b^n}{n!}F^n(a+\theta b),\ 0 < \theta < 1 \tag{2.22}$$

in which $F', F'', ..., F^n$ are the first, second, ..., n^{th} derivative of the F function, respectively. Last term is showing the remainder after n terms. Considering the remainder after two terms, the finite Taylor's series takes the form:

$$F(a+b) = F(a) + bF'(a) + \frac{b^2}{2!}F''(a+\theta b),\ 0 < \theta < 1 \tag{2.23}$$

13

Single Variable Function

Assume that $F(x) = 0$ is a single-variable nonlinear function and a is one of its roots so that $F(a) = 0$. An iterative procedure is required to find the value of a. If $_t\Delta x$ is additive correction for the tth iteration and $_tF(x)$ is the value of $F(x)$ at the tth iteration, the following equation may be written after the correction is applied.

$$F(x) = \ _tF(x + \Delta x) = 0 \tag{2.24}$$

If this equation is expanded as it is done in Equation 2.22, we obtain:

$$_tF(x) + \ _t\Delta x \cdot \ _tF'(x) + \frac{\left(_t\Delta x\right)^2}{2} \ _tF''(x + \theta\Delta x) = 0, \ 0 < \theta < 1 \tag{2.25}$$

In this equation, $_t\Delta x$ is a small value when comparing with $_tx$. Thus, $\left(_t\Delta x\right)^2$ is even a smaller value such that we can neglect the remainder after the first two terms. The new equation is as follows.

$$_tF'(x) \cdot \ _t\Delta x = - \ _tF(x) \tag{2.26}$$

$$_t\Delta x = - \ \left[\frac{F(x)}{F'(x)}\right]_t \tag{2.27}$$

The value of the next iteration is obtained as follows.

$$_{t+1}x = \ _tx + \ _t\Delta x = \ _tx - \ \left[\frac{F(x)}{F'(x)}\right]_t \tag{2.28}$$

If Equation 2.28 is used repeatedly, the root $x = a$ making $F(x) = 0$ is eventually found. If we consider Newton-Raphson Method in geometrical interpretation, $y = F(x)$, and if we want to draw a graph of it, it will be as in Figure 2.6.
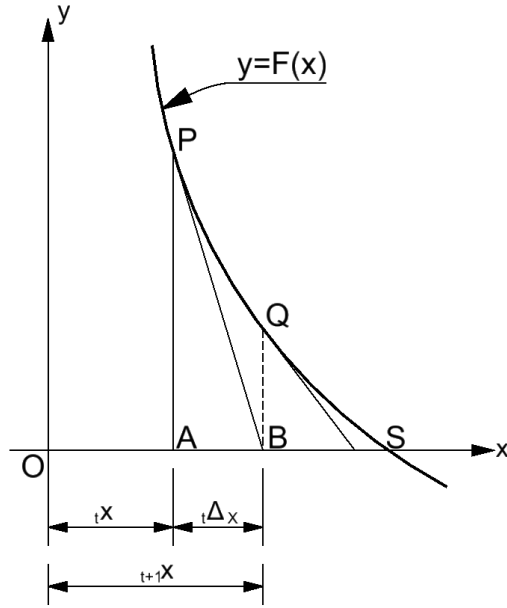
Figure 2.6: Geometrical Interpretation of the Newton-Raphson Method [6]

Multiple Variable Function

When Newton- Raphson Method is considered in multiple variable function, two equations can be given as follows.

$$F_1(x_1, x_2) = 0 \qquad (2.29)$$

and

$$F_2(x_1, x_2) = 0 \qquad (2.30)$$

Let the tth trial values of x_1, x_2, Δx_1, and Δx_2 be $_t x_1$, $_t x_2$, $_t \Delta x_1$, and $_t \Delta x_2$, respectively. As the same way with the single variable function, multiple variable function is as follows.

$$_t\left(\frac{\partial F_1}{\partial x_1}\right) \cdot {}_t\Delta x_1 + {}_t\left(\frac{\partial F_1}{\partial x_2}\right) \cdot {}_t\Delta x_2 = -{}_t F_1(x_1, x_2) \qquad (2.31)$$

$$_t\left(\frac{\partial F_2}{\partial x_1}\right) \cdot {}_t\Delta x_1 + {}_t\left(\frac{\partial F_2}{\partial x_2}\right) \cdot {}_t\Delta x_2 = -{}_t F_2(x_1, x_2) \qquad (2.32)$$

15

writing in the matrix form

$$
\left[\begin{matrix} \left(\frac{\partial F_1}{\partial x_1}\right) & \left(\frac{\partial F_1}{\partial x_2}\right) \\ \left(\frac{\partial F_2}{\partial x_1}\right) & \left(\frac{\partial F_2}{\partial x_2}\right) \end{matrix}\right]_t \left[\begin{matrix} \Delta x_1 \\ \Delta x_2 \end{matrix}\right]_t = - \left[\begin{matrix} F_1 \\ F_2 \end{matrix}\right]_t \tag{2.33}
$$

if we generalize this matrix form, it will be as follows.

$$
\left[\begin{matrix} \left(\frac{\partial F_1}{\partial x_1}\right) & \left(\frac{\partial F_1}{\partial x_2}\right) & \cdots & \left(\frac{\partial F_1}{\partial x_n}\right) \\ \left(\frac{\partial F_2}{\partial x_1}\right) & \left(\frac{\partial F_2}{\partial x_2}\right) & \cdots & \left(\frac{\partial F_2}{\partial x_n}\right) \\ \vdots & \vdots & \ddots & \vdots \\ \left(\frac{\partial F_n}{\partial x_1}\right) & \left(\frac{\partial F_n}{\partial x_2}\right) & \cdots & \left(\frac{\partial F_n}{\partial x_n}\right) \end{matrix}\right]_t \left[\begin{matrix} \Delta x_1 \\ \Delta x_2 \\ \vdots \\ \Delta x_n \end{matrix}\right]_t = - \left[\begin{matrix} F_1 \\ F_2 \\ \vdots \\ F_n \end{matrix}\right]_t \tag{2.34}
$$

The first matrix is called the coefficient matrix or the Jacobian of the n functions. The second matrix is the corrections column matrix and finally the column matrix on the other side of the equal sign is the residues of the functions $F_1, F_2, ..., F_n$. The iterations are performed until those values are sufficiently small.

2.1.4.3 Linear Theory Method

The nonlinearity in energy equations for pipe network is algebraic, uniform, and simple; the variables are raised to the same, non-unity exponent. For instance, nonlinear Q equations contain the nonlinear $k_{ij}Q_{ij}^n$ and the H equations, $[(H_i - H_j)/k_{ij}]^{1/n}$ with the same n values. It is 1.852 for Hazen-William (HW) head loss formula and 2.0 for Darcy-Weisbach (DW) and Manning head loss formula. This feature is useful since those nonlinear terms can be conveniently linearized by separating a part of the nonlinear term and putting it into the pipe resistance constant as in Equation 2.7. According to Bhave [6], this principle was first recommended and used by McIlroy [9], Marlow et al. [10], and Muir [11]. Later, Wood and Charles [12] developed this principle, and it is now widely used in practice. Although this principle can be used for all types of equations, it is used in practice for pipe discharge equations.

If we recall the nonlinear loop head-loss equation,

$$\sum_{pipe\ ij \in loop} (k_{ij}|_tQ_{ij}|^{n-1})Q_{ij} = 0 \qquad (2.35)$$

In which k_{ij} is the known pipe resistance constant, $_tQ_{ij}$ is assumed pipe discharge in the tth iteration step, and Q_{ij} is unknown pipe discharge. If this equation is linearized, it will be as follows.

$$\sum_{pipe\ ij \in loop} {}_tk'_{ij}Q_{ij} = 0 \qquad (2.36)$$

In which $_tk'_{ij}$ is the modified resistance constant of pipe ij in the tth iteration step and it stands for $k_{ij}|_tQ_{ij}|^{n-1}$.

Muir[11] and Wood and Charles [12] have recommended that the pipe discharge $_tQ_{ij}$ is set equal to 1 for the first iteration. Therefore, for the first iteration, $_1k'_{ij}$ is as follows.

$$_1k'_{ij} = k_{ij} \qquad (2.37)$$

If we rewrite Equation 2.36,

$$\sum_{pipe\ ij \in loop} k_{ij}Q_{ij} = 0 \qquad (2.38)$$

After that solutions of linear node-flow continuity equations and the linearized loop head loss equations together at the same time give us the pipe discharges $_2Q_{ij}$ in the loop at the end of the first iteration.

One can take the average of the assumed and obtained values in the previous iteration as $_tQ_{ij} = \frac{(t-1)Q_{ij}+{}_tQ_{ij}}{2}$ to find the pipe discharge at the tth iteration. This is leading to rapid convergence.

CHAPTER 3

NUMERICAL MODEL: THE FINITE ELEMENT METHOD

In the previous chapter, three numerical solutions for analyzing pipe networks, namely Hardy Cross method, Newton-Raphson method, Linear Theory method, were explained.

In addition to these numerical solution methods, the Finite Element Modeling (FEM) is also used to analyze pipe networks. The advantage of the FEM its easiness to be programmed in a computer language. Also it helps the analyzer to add or remove an element in a network conveniently. Like in Linear Theory Method, the aim of FEM is also showing the head loss term in a general form which is $k_{ij}Q^n$. According to Mohtar et al. [5], expressing the loss terms in a common form for all the pipe components will help the finite element formulation for analyzing pipe networks. Next, the head loss term will be explained for each type of element in pipe network analysis.

3.1   Head Loss Formulation

Head losses are divided into two groups. These are major losses and minor losses. They are also called friction losses and local losses, respectively. Formulation of these head losses will be explained in detail for different elements.

3.1.1 Pipe Element Head Loss Formulation for Friction Losses

Pipe element and its finite element representation is shown in Figure 3.1. Pipe element head losses are known as major head losses. Typically, there are two types of friction head loss formula for pipe elements. These are Hazen-William and Darcy-Weisbach equations.
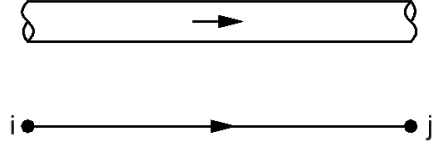
Figure 3.1: General Pipe Element ij and its Finite Element Representation

3.1.1.1 Hazen-William Head Loss Formula for Friction Losses

It is basically as follows.

$$h_{l(pipe)} = \frac{K_{pipe}LQ_{ij}^n}{C_{HW}^n D^m} \tag{3.1}$$

Where K_{pipe} is a constant equal to 10.68, C is a Hazen-William friction coefficient, L is the pipe length in meter, D is the pipe diameter in meter, Q_{ij} is the pipe discharge in meter cube per second, and n and m are constants with a value of 1.852 and 4.87, respectively.

Hazen-William head loss formula can be written as follows.

$$h_{l(pipe)} = k_{ij}Q_{ij}^n \tag{3.2}$$

Where k_{ij} stands for $\frac{K_{pipe}L}{C_{HW}^m D^m}$.

3.1.1.2 Darcy-Weisbach Head Loss Formula

Darcy-Weisbach head loss formula is expressed as follows.

$$h_{l(pipe)} = f\frac{L}{D}\frac{V^2}{2g} \tag{3.3}$$

Where f is the Darcy-Weisbach friction factor that is explained below, L is the pipe length in meter, D is the pipe diameter in meter, V is the velocity of the fluid in meter per second, and g is the gravitational acceleration in meter per

second squared.

Darcy-Weisbach friction factor (f) can be found by Colebrook-White formula [13]. It is as follows.

$$\frac{1}{\sqrt{f}} = -2\log_{10}\left[\frac{\varepsilon}{3.7D} + \frac{2.51}{Re\sqrt{f}}\right] \tag{3.4}$$

Where ε is the roughness height of the pipe wall in meter, D is the pipe diameter in meter, Re is the dimensionless Reynolds Number expressed below.

$$Re = \frac{VD}{\nu} \tag{3.5}$$

Where D is the pipe diameter in m, V is the velocity of the fluid in meter per second, ν is the kinematic viscosity of the fluid in meter squared per second.

Since Colebrook-White equation is nonlinear equation and it needs the iterative solution for finding the friction factor f. Colebrook equation [14] for assuming hydraulically rough flow ($Re \geq 4000$) may be used for the first trial friction factors. It is shown below.

$$f = \frac{1.325}{ln\left(\frac{\epsilon}{3.7D}\right)^2} \tag{3.6}$$

Where ε is the roughness height of the pipe wall in meter, D is the pipe diameter in meter.

Head loss formula of Darcy-Weisbach can be written in terms of discharge as

$$h_{l(pipe)} = \frac{8fL}{g\pi^2 D^5}Q_{ij}^2 \tag{3.7}$$

This can be further expressed as

$$h_{l(pipe)} = k_{ij}Q_{ij}^n \tag{3.8}$$

Where k_{ij} stands for $\frac{8fL}{g\pi^2 D^5}$ and n is 2.0.

3.1.2 Pipe Fitting Element Head Loss Formulation for Local Losses

Most commonly used pipe fitting elements are bends, tees, contraction and expansion in pipe area, and valves. These elements would generate head loss locally, wherever they exist. These are shown in Figure 3.2. A general head loss
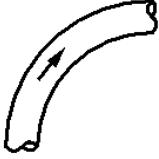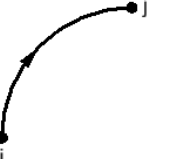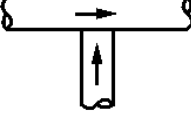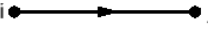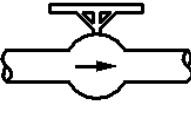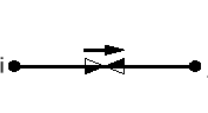
Figure 3.2: General Fitting Elements and their Finite Element Representations

formula of pipe fittings is as follows.

$$h_{l(fitting)} = K_{fitting}\frac{V^2}{2g} \tag{3.9}$$
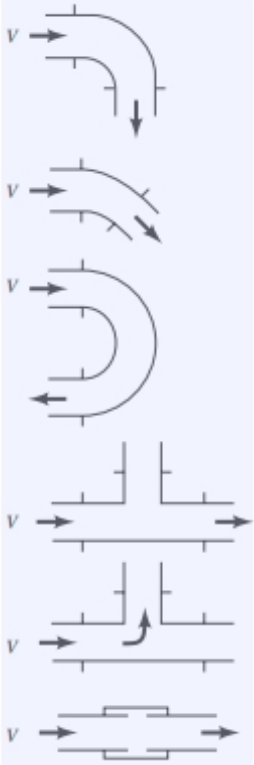
Where $K_{fitting}$ is a fitting loss coefficient, which is different for each type of fitting element, V is the average velocity of the fluid in meter per second, and g is the gravitational acceleration in meter per second squared .

Fitting head loss formula can be written as follows.

$$h_{l(fitting)} = k_{ij}Q_{ij}^n \tag{3.10}$$

where k_{ij} stands for $\frac{K_{fitting}}{2gA^2}$ and n is 2.0.

Fitting Coefficient ($K_{fitting}$) has a specific value for all type of fitting elements. For example, in the network system, there may be a lot of valves or bends. For each type of valve or bend, there is a certain fitting coefficient. Some of these fitting coefficients are listed in Figure 3.3.

a. Elbows

Regular 90°, flanged	0.3
Regular 90°, threaded	1.5
Long radius 90°, flanged	0.2
Long radius 90°, threaded	0.7
Long radius 45°, flanged	0.2
Regular 45°, threaded	0.4

b. 180° return bends

180° return bend, flanged	0.2
180° return bend, threaded	1.5

c. Tees

Line flow, flanged	0.2
Line flow, threaded	0.9
Branch flow, flanged	1.0
Branch flow, threaded	2.0

d. Union, threaded — 0.08

*e. Valves

Globe, fully open	10
Angle, fully open	2
Gate, fully open	0.15
Gate, $\frac{1}{4}$ closed	0.26
Gate, $\frac{1}{2}$ closed	2.1
Gate, $\frac{3}{4}$ closed	17
Swing check, forward flow	2
Swing check, backward flow	∞
Ball valve, fully open	0.05
Ball valve, $\frac{1}{3}$ closed	5.5
Ball valve, $\frac{2}{3}$ closed	210

*See Fig. 8.36 for typical valve geometry

Figure 3.3: Fitting Coefficients [13]

If the fitting is contraction, there is a fitting coefficient graph shown in Figure 3.4. As it is seen in Figure 3.4, fitting coefficient is changing with the ratio of the pipe areas. In order to get rid of measuring the fitting coefficient for the pipeline system and to be used in the written program, it is formulated as shown below.

$$K_{fitting}\left(\frac{A_j}{A_i}\right) = -2.6042\left(\frac{A_j}{A_i}\right)^5 + 6.7708\left(\frac{A_j}{A_i}\right)^4 - 5.3125\left(\frac{A_j}{A_i}\right)^3 +$$

$$0.9792\left(\frac{A_j}{A_i}\right)^2 - 0.3333\left(\frac{A_j}{A_i}\right) + 0.5 \quad (3.11)$$
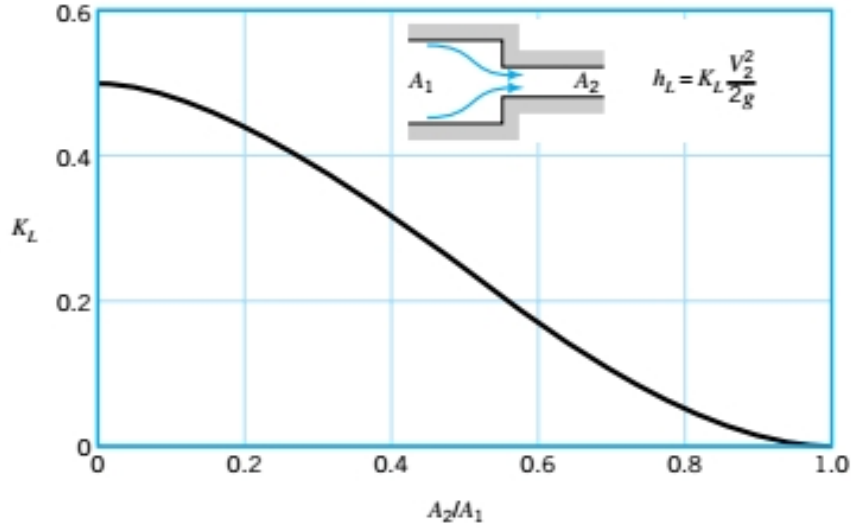
Figure 3.4: Loss coefficient for a sudden contraction [13]

Where A_i and A_j stands for area of the ith and j^{th} node, respectively.
If the fitting is expansion, Swamee [14] set the $K_{fitting}$ equal to 1.0 .

3.1.3 Pump Pressure Head Formulation

Pump element and its finite element representation is shown in Figure 3.5.
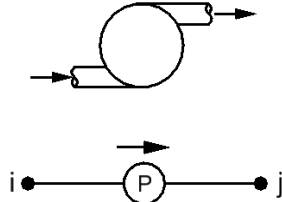
Figure 3.5: General Pump Element and its Finite Element Representation

The typical characteristic curve of a centrifugal booster pump may be expressed
as in Equations (3.2-3.12), Mohtar et al. [5].

$$h_{l(pump)} = COH - aQ_{ij}^b \tag{3.12}$$

Where COH is the cut of head that represents the pressure head at zero flow
when the valve is closed on the discharge side of the pump. a and b are constants
of pump characteristics curve. COH is a constant positive term to be added
to the elevation of the downstream node of the pump element. Therefore, the

24

pump head takes the form

$$h_{l(pump)} = k_{ij} Q_{ij}^n \tag{3.13}$$

Where $k_{ij} = -a$ and $n = b$. The reason k_{ij} is negative is that energy is being added to the system.

3.2 General Finite Element Formulation

Consider an element in a network and assume flow direction is from i^{th} node to j^{th} node shown in Figure 3.6. If we write the energy equation for this element,

Figure 3.6: General Finite Element for Pipes

it will be as follows.

$$\frac{P_i}{\gamma} + Z_i + \frac{V_i^2}{2g} = \frac{P_j}{\gamma} + Z_j + \frac{V_j^2}{2g} + k_{ij} Q_{ij}^n \tag{3.14}$$

Where k_{ij} is the resistance constant, Q_{ij} is the element discharge, P_i/γ, Z_i, $V_i^2/2g$ are pressure head, elevation head, and kinetic energy head at the ith node and P_j/γ, Z_j, $V_j^2/2g$ are pressure head, elevation head, and kinetic energy head at the jth node, respectively.

If we rearrange Equation 3.14, it will become,

$$\frac{P_i}{\gamma} + Z_i + \frac{Q_{ij}^2}{A_i^2 2g} = \frac{P_j}{\gamma} + Z_j + \frac{Q_{ij}^2}{A_j^2 2g} + k_{ij} Q_{ij}^n \tag{3.15}$$

where V^2 is equal to Q_{ij}^2/A^2.

Equation 3.15 can be written as follows.

$$\left(\frac{P_i}{\gamma} - \frac{P_j}{\gamma} \right) + (Z_i - Z_j) = k_{ij} Q_{ij}^n - \frac{Q_{ij}^2}{2g} \left(\frac{1}{A_i^2} - \frac{1}{A_j^2} \right) \tag{3.16}$$

or

$$\left(\frac{P_i}{\gamma} - \frac{P_j}{\gamma} \right) + (Z_i - Z_j) = \left[k_{ij} - \frac{1}{2g Q_{ij}^{n-2}} \left(\frac{1}{A_i^2} - \frac{1}{A_j^2} \right) \right] Q_{ij}^n \tag{3.17}$$

if we take Q_{ij} term alone, it will be as follows.

$$Q_{ij} = \frac{\left[\left(\frac{P_i}{\gamma} - \frac{P_j}{\gamma} \right) + (Z_i - Z_j) \right]^{1/n}}{\left[k_{ij} - \frac{1}{2g Q_{ij}^{n-2}} \left(\frac{1}{A_i^2} - \frac{1}{A_j^2} \right) \right]^{1/n}} \tag{3.18}$$

This equation is put in a form for a matrix structure as below.

$$Q_{ij} = \frac{\left[\left(\frac{P_i}{\gamma} - \frac{P_j}{\gamma}\right) + (Z_i - Z_j)\right]^{\frac{(1-n)}{n}}}{\left[k_{ij} - \frac{1}{2gQ_{ij}^{n-2}}\left(\frac{1}{A_i^2} - \frac{1}{A_j^2}\right)\right]^{1/n}} \left[\left(\frac{P_i}{\gamma} - \frac{P_j}{\gamma}\right) + (Z_i - Z_j)\right] \qquad (3.19)$$

This equation may be written as

$$Q_{ij} = C_{ij}\left(\frac{P_i}{\gamma} - \frac{P_j}{\gamma}\right) + C_{ij}(Z_i - Z_j) \qquad (3.20)$$

where C_{ij} stands for $\dfrac{\left[\left(\frac{P_i}{\gamma} - \frac{P_j}{\gamma}\right) + (Z_i - Z_j)\right]^{\frac{(1-n)}{n}}}{\left[k_{ij} - \frac{1}{2gQ_{ij}^{n-2}}\left(\frac{1}{A_i^2} - \frac{1}{A_j^2}\right)\right]^{1/n}}$

Rewriting the equation in a matrix formulation

$$_t\begin{bmatrix} Q_i^{(e)} \\ Q_j^{(e)} \end{bmatrix} = {}_tC_{ij}\begin{bmatrix} +1 & -1 \\ -1 & +1 \end{bmatrix}_{t+1}\begin{bmatrix} P_i^{(e)}/\gamma \\ P_j^{(e)}/\gamma \end{bmatrix} + {}_tC_{ij}\begin{bmatrix} (Z_i - Z_j)^{(e)} \\ -(Z_i - Z_j)^{(e)} \end{bmatrix} \qquad (3.21)$$

or

$$_t\left[Q^{(e)}\right] = {}_t\left[K^{(e)}\right]_{t+1}\left[P/\gamma^{(e)}\right] + {}_t\left[\Delta_Z^{(e)}\right] \qquad (3.22)$$

or

$$_t\left[K^{(e)}\right]_{t+1}\left[P/\gamma^{(e)}\right] = {}_t\left[Q^{(e)}\right] - {}_t\left[\Delta_Z^{(e)}\right] \qquad (3.23)$$

where (e) represents the element number and t is the iteration step.

At each iteration, a linear system of equations of size is same as the number of nodes in the network. This matrix form is illustrated just for one element. For the entire system, all elements' equations are assembled. We generalize this element matrix for the whole system of a network. If all element equations are assembled, Equation 3.23 will be as follows.

$$_t\left[K\right]_{t+1}\left[P/\gamma\right] = {}_t\left[Q\right] - {}_t\left[\Delta_Z\right] \qquad (3.24)$$

As it is seen in Equation 3.24, both $\left[K\right]$ and $\left[P/\gamma\right]$ terms are functions of pressure head (P/γ). This Equation is an implicit equation because some of (P/γ) terms are unknown in pipe network. Therefore, in the first iteration, unknown $_t\left[P/\gamma\right]$ values in $\left[K\right]$ are assumed and elements' flow directions for the first iteration is constructed. Then, the unknown P/γ values in $_{t+1}\left[P/\gamma\right]$ are found. Those $_{t+1}\left[P/\gamma\right]$ values, which are obtained at the end of the first iteration, are

used as input P/γ values for the matrix $\begin{bmatrix} K \end{bmatrix}$ for the second iteration and so on. Iterations proceed until $\dfrac{_{t+1}(P/\gamma) - {_t}(P/\gamma)}{_t(P/\gamma)}$ is small enough. In this way, P/γ values and accordingly element discharges can be found. Furthermore, the Equation 3.24 cannot be calculated because $\begin{bmatrix} K \end{bmatrix}$ matrix is a singular matrix without the boundary conditions. In order to get rid of this situation, the boundary conditions must be applied. The Row-Column Elimination is is preferred approach in imposing the boundary conditions on P/γ values. It is expressed next.

3.2.1 Row-Column Elimination

Equation 3.24 may be simply rewritten as follows.

$$Ku = f \tag{3.25}$$

According to Reddy [15], if we write Equation 3.25 more explicitly, it is as follows.

$$
\begin{bmatrix}
K_{11} & K_{12} & K_{13} & \dots & K_{1n} \\
K_{21} & K_{22} & K_{23} & \dots & K_{2n} \\
K_{31} & K_{32} & K_{33} & \dots & K_{3n} \\
\vdots & \vdots & \vdots & \ddots & \vdots \\
K_{n1} & K_{n2} & K_{n3} & \dots & K_{nn}
\end{bmatrix}
\begin{bmatrix}
u_1 \\ u_2 \\ u_3 \\ \vdots \\ u_n
\end{bmatrix}
=
\begin{bmatrix}
f_1 \\ f_2 \\ f_3 \\ \vdots \\ f_n
\end{bmatrix}
\tag{3.26}
$$

If we use α instead of a known essential boundary condition u_2 and substitute α into Equation 3.26, the equation will form as follows.

$$
\begin{bmatrix}
K_{11} & K_{12} & K_{13} & \dots & K_{1n} \\
0 & 1 & 0 & \dots & 0 \\
K_{31} & K_{32} & K_{33} & \dots & K_{3n} \\
\vdots & \vdots & \vdots & \ddots & \vdots \\
K_{n1} & K_{n2} & K_{n3} & \dots & K_{nn}
\end{bmatrix}
\begin{bmatrix}
u_1 \\ u_2 \\ u_3 \\ \vdots \\ u_n
\end{bmatrix}
=
\begin{bmatrix}
f_1 \\ \alpha \\ f_3 \\ \vdots \\ f_n
\end{bmatrix}
\tag{3.27}
$$

Equation 3.27 can be further modified as follows.

$$
\begin{bmatrix}
K_{11} & 0 & K_{13} & \dots & K_{1n} \\
0 & 1 & 0 & \dots & 0 \\
K_{31} & 0 & K_{33} & \dots & K_{3n} \\
\vdots & \vdots & \vdots & \ddots & \vdots \\
K_{n1} & 0 & K_{n3} & \dots & K_{nn}
\end{bmatrix}
\begin{bmatrix}
u_1 \\ u_2 \\ u_3 \\ \vdots \\ u_n
\end{bmatrix}
=
\begin{bmatrix}
f_1 \\ \alpha \\ f_3 \\ \vdots \\ f_n
\end{bmatrix}
- \alpha
\begin{bmatrix}
K_{12} \\ 0 \\ K_{32} \\ \vdots \\ K_{n2}
\end{bmatrix}
\tag{3.28}
$$

This approach is more systematic then the row and column reordering method which is less frequently used. It preserves symmetry and avoids singularity.

In this way, $\left[K\right]$ matrix may be inverted. Apart from the general formulation of FEM for pipeline system, construction of C_{ij} formulation may vary for different type of the pipeline system elements. This construction of C_{ij} formulation for a different type of element is expressed in detail below.

3.3 Formulation of C_{ij} for Different Elements

3.3.1 Formulation of C_{ij} for Pipe Element

As it is mentioned before, the general C_{ij} formulation is as follows.

$$C_{ij} = \frac{\left[\left(\frac{P_i}{\gamma} - \frac{P_j}{\gamma}\right) + (Z_i - Z_j)\right]^{\frac{(1-n)}{n}}}{\left[k_{ij} - \frac{1}{2gQ_{ij}^{n-2}}\left(\frac{1}{A_i^2} - \frac{1}{A_j^2}\right)\right]^{1/n}} \tag{3.29}$$

In general, a pipe element has a constant pipe diameter (D). In other words, areas of the ith node and j^{th} node are the same in a pipe element. Therefore, the general formulation of the C_{ij} may be simplified for the pipe element and it is given below.

$$C_{ij} = \frac{\left[\left(\frac{P_i}{\gamma} - \frac{P_j}{\gamma}\right) + (Z_i - Z_j)\right]^{\frac{(1-n)}{n}}}{[k_{ij}]^{1/n}} \tag{3.30}$$

As it is easily seen from the equation, area terms are canceled out and the C_{ij} formulation is simplified for the pipe element.

For a pipe element, the value of exponent m depends on whether or not Hazen-William head loss formula or Darcy-Weisbach head loss formula is used.

Rewriting the C_{ij} formulation of pipe element according to Hazen-William head loss formula with $n = 1.852$.

$$C_{ij} = \frac{\left[\left(\frac{P_i}{\gamma} - \frac{P_j}{\gamma}\right) + (Z_i - Z_j)\right]^{\frac{(1-1.852)}{1.852}}}{[k_{ij}]^{1/1.852}} \tag{3.31}$$

28

Rewriting the C_{ij} formulation of pipe element according to Darcy-Weisbach head loss formula with $n = 2.0$.

$$C_{ij} = \frac{\left[\left(\frac{P_i}{\gamma} - \frac{P_j}{\gamma}\right) + (Z_i - Z_j)\right]^{\frac{(1-2.0)}{2.0}}}{[k_{ij}]^{1/2.0}} \qquad (3.32)$$

3.3.2 Formulation of C_{ij} for Fitting Element

Fitting elements may be grouped in two parts. While the first group may be composed of bends, tees, valves, the second group may be considered as contraction and expansion in pipe area. As the area of the ith node and the jth node are the same for the first group fittings, the C_{ij} formulation is the same as that for the pipe element. It is shown below.

$$C_{ij} = \frac{\left[\left(\frac{P_i}{\gamma} - \frac{P_j}{\gamma}\right) + (Z_i - Z_j)\right]^{\frac{(1-n)}{n}}}{[k_{ij}]^{1/n}} \qquad (3.33)$$

Rewriting the equation for $n = 2.0$ for fitting elements

$$C_{ij} = \frac{\left[\left(\frac{P_i}{\gamma} - \frac{P_j}{\gamma}\right) + (Z_i - Z_j)\right]^{\frac{(1-2.0)}{2.0}}}{[k_{ij}]^{1/2.0}} \qquad (3.34)$$

In the second group which includes contractions and expansions, the area of the ith node is different from the area of the jth node. At this point, we have to go back to the head loss formulation for contraction and expansion. Recall the head loss formulation shown below.

$$h_{l(fitting)} = K_{fitting}\frac{V^2}{2g} \qquad (3.35)$$

Because of the variation in areas for i^{th} and j^{th} node, velocity of the fluid is different at i^{th} and j^{th} node. Therefore, the head loss formulation is rewritten as follows.

$$h_{l(fitting)} = K_{fitting}\frac{\left(\frac{V_i + V_j}{2}\right)^2}{2g} = K_{fitting}\frac{(V_i + V_j)^2}{8g} \qquad (3.36)$$

Rewriting the equation for $V_i = \frac{Q_{ij}}{A_i}$ and $V_j = \frac{Q_{ij}}{A_j}$

$$h_{l(fitting)} = K_{fitting}\frac{\left(\frac{Q_{ij}}{A_i} + \frac{Q_{ij}}{A_j}\right)^2}{8g} = \frac{K_{fitting}}{8g}\left(\frac{A_i + A_j}{A_i A_j}\right)^2 Q_{ij}^2 \qquad (3.37)$$

If the head loss formulation is generalized, it will be as follows.

$$h_{l(fitting)} = k_{ij}Q_{ij}^n \tag{3.38}$$

Where $k_{ij} = \dfrac{K_{fitting}}{8g}\left(\dfrac{A_i + A_j}{A_iA_j}\right)^2$ and $n = 2.0$

Next, if we write the energy equation from the ith node to the jth node

$$\frac{P_i}{\gamma} + Z_i + \frac{V_i^2}{2g} = \frac{P_j}{\gamma} + Z_j + \frac{V_j^2}{2g} + k_{ij}Q_{ij}^n \tag{3.39}$$

Rewriting the equation for $V_i = \dfrac{Q_{ij}}{A_i}$, $V_j = \dfrac{Q_{ij}}{A_j}$, $k_{ij} = \dfrac{K_{fitting}}{8g}\left(\dfrac{A_i + A_j}{A_iA_j}\right)^2$ and $n = 2.0$

$$\frac{P_i}{\gamma} + Z_i + \frac{\left(\dfrac{Q_{ij}}{A_i}\right)^2}{2g} = \frac{P_j}{\gamma} + Z_j + \frac{\left(\dfrac{Q_{ij}}{A_j}\right)^2}{2g} + \frac{K_{fitting}}{8g}\left(\frac{A_i + A_j}{A_iA_j}\right)^2 Q_{ij}^{2.0} \tag{3.40}$$

If Q_{ij} term in Equation 3.40 is taken alone, it will be as follows.

$$Q_{ij} = \left[\frac{\left(\frac{P_i}{\gamma} - \frac{P_j}{\gamma}\right) + (Z_i - Z_j)}{\left(\dfrac{4A_i^2 - 4A_j^2 + K(A_i + A_j)}{8gA_i^2A_j^2}\right)}\right]^{\frac{1}{2}} \tag{3.41}$$

Where $K = K_{fitting}$, but the word fitting was not kept for the sake of conveniency. If this equation is reformed in a suitable matrix structure, it will be as follows.

$$Q_{ij} = \left[\frac{\left(\frac{P_i}{\gamma} - \frac{P_j}{\gamma}\right) + (Z_i - Z_j)}{\left(\dfrac{4A_i^2 - 4A_j^2 + K(A_i + A_j)}{8gA_i^2A_j^2}\right)}\right]^{\frac{1}{2}} \left(\frac{1}{\left(\frac{P_i}{\gamma} - \frac{P_j}{\gamma}\right) + (Z_i - Z_j)}\right)$$
$$\left[\left(\frac{P_i}{\gamma} - \frac{P_j}{\gamma}\right) + (Z_i - Z_j)\right] \tag{3.42}$$

Hereby, C_{ij} is constructed for contraction and expansion and it is as follows.

$$C_{ij} = \left[\frac{\left(\frac{P_i}{\gamma} - \frac{P_j}{\gamma}\right) + (Z_i - Z_j)}{\left(\dfrac{4A_i^2 - 4A_j^2 + K(A_i + A_j)}{8gA_i^2A_j^2}\right)}\right]^{\frac{1}{2}} \left(\frac{1}{\left(\frac{P_i}{\gamma} - \frac{P_j}{\gamma}\right) + (Z_i - Z_j)}\right) \tag{3.43}$$

30

3.3.3 Formulation of C_{ij} for Pump Element

Energy equation is written for a pump element as shown below.

$$\frac{P_i}{\gamma} + Z_i + \frac{V_i^2}{2g} = \frac{P_j}{\gamma} + Z_j + \frac{V_j^2}{2g} - (COH + k_{ij}Q_{ij}^n) \tag{3.44}$$

Because of the areas of the ith and j^{th} node are the same, kinetic energy term will be cancelled each other. Then, we rewrite the equation for $k_{ij} = -a$ and $n = b$

$$\frac{P_i}{\gamma} + Z_i = \frac{P_j}{\gamma} + Z_j - COH + aQ_{ij}^b \tag{3.45}$$

If Q_{ij} term is taken alone, it will be as follows.

$$Q_{ij} = \left[\frac{\left(\frac{P_i}{\gamma} - \frac{P_j}{\gamma}\right) + (Z_i - Z_j) + COH}{a}\right]^{\frac{1}{b}} \tag{3.46}$$

Rewriting the equation for a suitable matrix form

$$Q_{ij} = \left[\frac{\left(\frac{P_i}{\gamma} - \frac{P_j}{\gamma}\right) + (Z_i - Z_j) + COH}{a}\right]^{\frac{1}{b}} \left(\frac{1}{\left(\frac{P_i}{\gamma} - \frac{P_j}{\gamma}\right) + (Z_i - Z_j) + COH}\right)$$
$$\left[\left(\frac{P_i}{\gamma} - \frac{P_j}{\gamma}\right) + (Z_i - Z_j) + COH\right] \tag{3.47}$$

Hereby, C_{ij} is constructed and it is shown below.

$$C_{ij} = \left[\frac{\left(\frac{P_i}{\gamma} - \frac{P_j}{\gamma}\right) + (Z_i - Z_j) + COH}{a}\right]^{\frac{1}{b}} \left(\frac{1}{\left(\frac{P_i}{\gamma} - \frac{P_j}{\gamma}\right) + (Z_i - Z_j) + COH}\right)$$
$$\tag{3.48}$$

Besides, it is easily seen here, it has to be explained that our matrix equation has one more vector matrix $[COH]$. Thus, our matrix formulation for pumps is as follows.

$$\begin{bmatrix} Q_i^{(e)} \\ Q_j^{(e)} \end{bmatrix}_t = {}_tC_{ij} \begin{bmatrix} +1 & -1 \\ -1 & +1 \end{bmatrix}_{t+1} \begin{bmatrix} P_i^{(e)}/\gamma \\ P_j^{(e)}/\gamma \end{bmatrix} + {}_tC_{ij} \begin{bmatrix} (Z_i - Z_j)^{(e)} \\ -(Z_i - Z_j)^{(e)} \end{bmatrix} + {}_tC_{ij} \begin{bmatrix} COH^{(e)} \\ -COH^{(e)} \end{bmatrix} \tag{3.49}$$

If COH term in Equation 3.46 is added directly to the $(Z_i - Z_j)$ term and then construct the matrix form, the results of the problems would be wrong due to the nonlinearity in the energy equation. Therefore, $[COH]$ vector matrix has to appear separately in Equation 3.49.

3.4 Solution Methods of System of Linear Equations

There are several solution methods for the solution of the system of equations. These are generally classified in two categories as direct and iterative methods. Among the direct solution methods, Gaussian elimination and LU decomposition methods are the most popular. Among the iterative methods, Gauss-Seidel and Conjugate Gradient methods are popular. In the thesis, LU decomposition as a direct solution method and Conjugate Gradient method as an iterative method are used. This will be explained next.

3.4.1 LU Decomposition Method (Direct)

This method is the simplest method. It simply solves $Ku = f$ equation by using LU decomposition. In this method, system matrix (K) is inverted and directly multiplied with the vector f as shown below.

$$K^{-1}f = u \tag{3.50}$$

This version is usually achieved by elimination techniques. This method may be useful while mesh size could be up to the thousands. However, it will be convenient when we have millions of nodes in the network because of the required memory and computer times. Thus, conjugate gradient method becomes a preferred approach.

3.4.2 Conjugate Gradient Method(Iterative)

This method also solves $Ku = f$ equation. However, while there may be millions of meshes in pipe network, this method converges to the solution faster than the direct solution method because iteration steps are less than the direct solution method.

Steps of conjugate gradient method for the symmetric and positive defined matrix K according to Dai et al. [16] are as follows.

$$p_0 = r_0 = k - Ku_0 \quad (u_0 \ arbitrary)$$

Let us say $i = 0$.

Repeat

$$Step1: \quad \alpha_i = \frac{r_i^T r_i}{p_i^T A p_i}$$

$$Step2: \quad u_{i+1} = u_i + \alpha_i p_i$$

$$Step3: \quad r_{i+1} = r_i - \alpha_i K p_i \qquad if\ r_{i+1} \approx 0,\ then\ stop$$

$$Step4: \quad \beta_i = \frac{r_{i+1}^T r_{i+1}}{r_i^T r_i}$$

$$Step5: \quad p_{i+1} = r_{i+1} + \beta_i p_i$$

CHAPTER 4

DEVELOPMENT OF SOFTWARE

In this chapter, the environment of the program, logic of the program, and input and output generation of the program will be expressed.

The program was written in Fortran F95 programming language. While developing the program, a support was received from NetBeans Integrated Development Environment (IDE) 8.1. Apart from these, C++ programming language and QT cross-platform application framework [17] have been used to develop the developed graphical user interface (GUI) for integrating the program into the $CAEeda^{TM}$ software package by EDA Ltd. company.

4.1 The Input Generation For The Program

The input file to be used by the program is created by using Geometry and Preprocess modules of $CAEeda^{TM}$. User draws a sketch for the pipeline network using the Geometry module and then firstly identifies different types of elements of his network using the Prepocess module.

The network topology is exported by $CAEeda^{TM}$ as a FEM type line mesh file with an extension of ".edf". The other necessary inputs involving solution type, loss modeling type, solution accuracy and desired output details are entered to the program by means of an other input file with an extension of ".inp". This file is generated by an graphical user interface as shown in Figure 4.1.
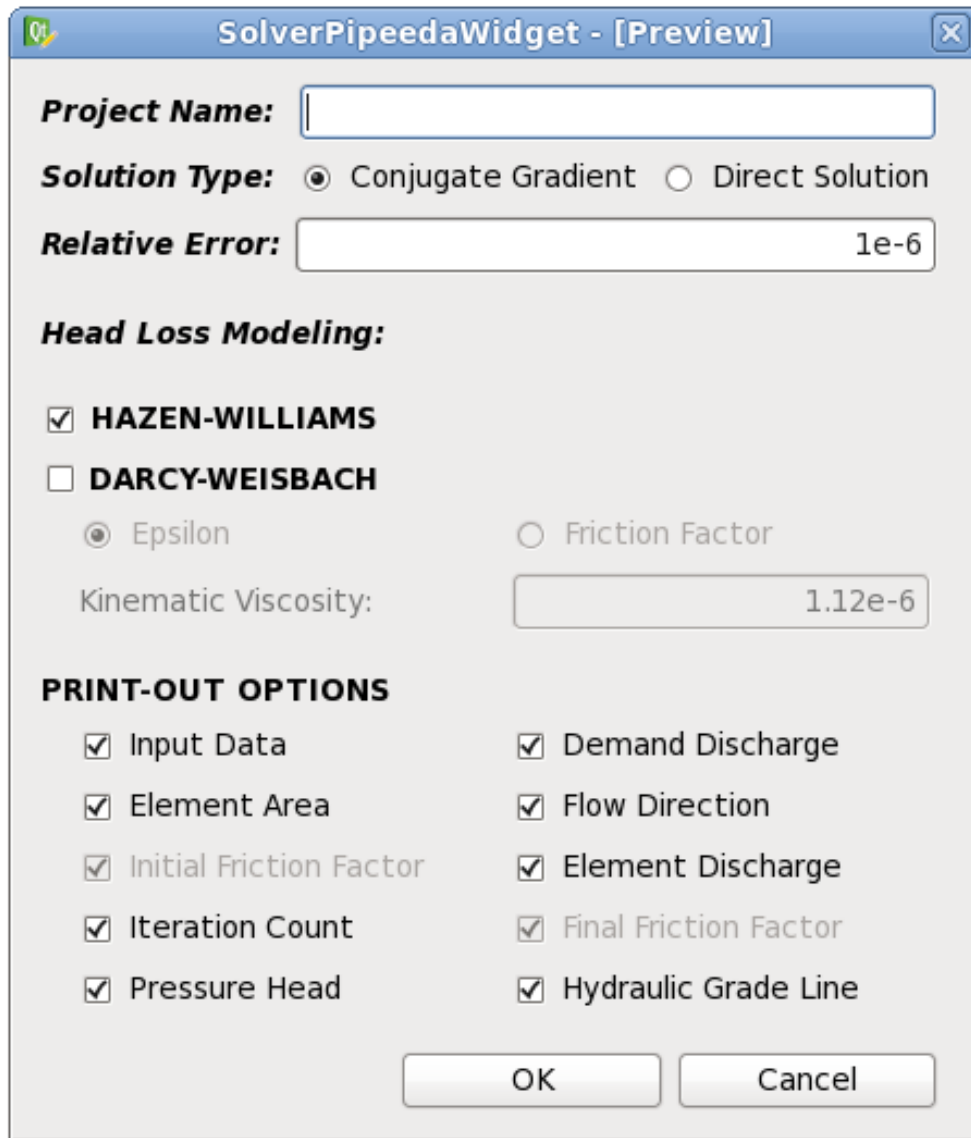
Figure 4.1: The Graphical User Interface integrated to $CAEeda^{TM}$

Program process is basically shown in Figure 4.2. The user follows the geometry, preprocess, solver gui section and enter all of the data.
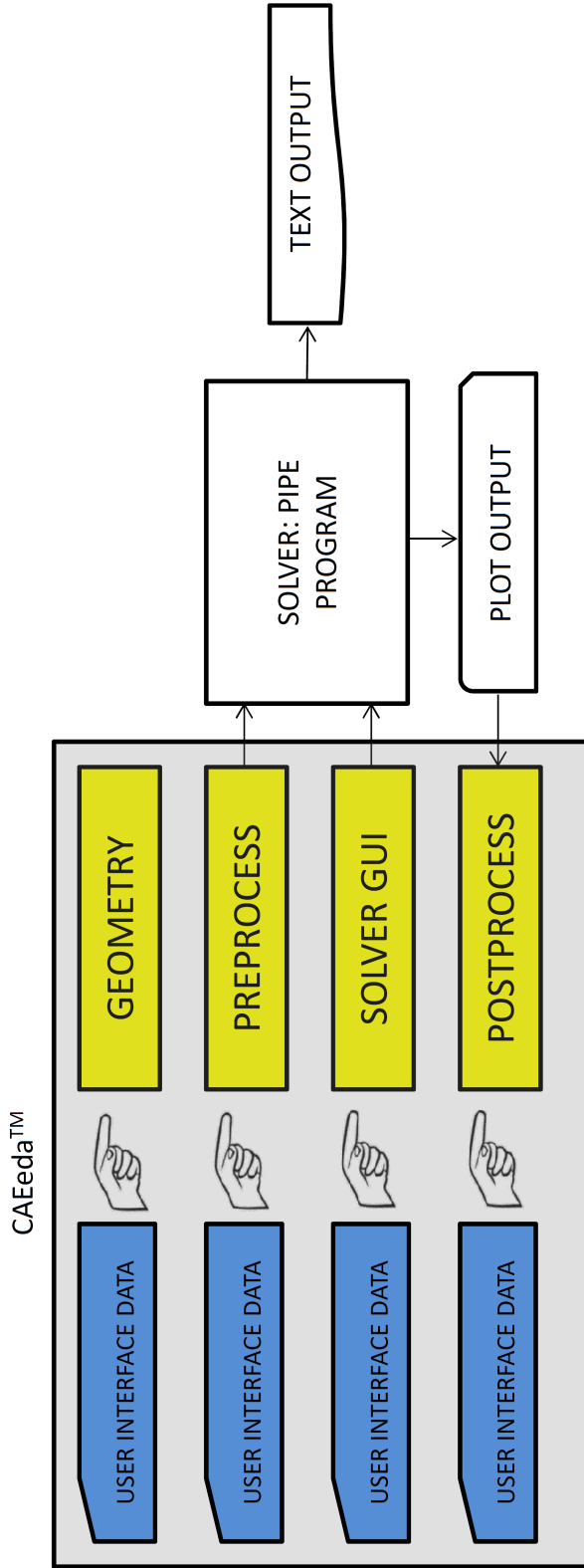
Figure 4.2: The Pipe Network Solution Process ($CAEeda^{TM}$ - Pipe Program Interaction)

After entering all data in the geometry, preprocess section, the input file is generated. Input file is divided into six parts.

In the first part, it contains node, element, and zone number of the designed pipeline network. It is shown in Figure 4.3.

```
nnodes nlines nzones
17 19 12
```

Figure 4.3: Number of Nodes, Elements and Zones in Input

In the second part, the zones are defined. The zones are useful when designing a network because user can use the same element or same nodal information applicable to the different parts of the pipeline network. In other words, a zone is used such that the user does not have to redefine the same structure through the different parts of the pipeline network. It is shown in Figure 4.4.

```
ZONES
id type name bc material thickness bodytype
1 N "reservoir" 40 1 -1.00000000 N
2 N "discharge" 39 1 -1.00000000 N
3 N "discharge-2" 39 1 -1.00000000 N
4 L "pipe1" 35 1 -1 N
5 L "valve" 36 1 -1 N
6 L "pump" 38 1 -1 N
7 N "reservoir-2" 40 1 -1.00000000 N
8 N "reservoir-3" 40 1 -1.00000000 N
9 N "reservoir-4" 40 1 -1.00000000 N
10 N "discharge-3" 39 1 -1.00000000 N
11 N "discharge-4" 39 1 -1.00000000 N
12 N "discharge-5" 39 1 -1.00000000 N
```

Figure 4.4: Definition of Zone IDs, Types, Names, Boundary Conditions, Materials, Thickness in Input

Furthermore, the third part is nodes with the geographical coordinates (x, y, z) and relevant zone label. It is illustrated in Figure 4.5.

```
NODES
id x y z zone
1  -90124.583  17769.232 3.00000000 1
2  -91553.186  20598.066 30.00000000 1
3  -91919.857  20017.137 34.00000000 1
4  -91823.029  20047.795 34.00000000 1
5  -90125.030  17770.127 3.00000000 2
6  -90796.040  19112.761 12.00000000 4
7  -91556.034  19112.761 15.00000000 4
8  -90796.032  19723.744 12.00000000 4
9  -90796.032  20637.725 18.00000000 4
10 -91553.186  20572.085 15.00000000 4
11 -91339.514  20000.739 12.00000000 4
12 -91787.643  20090.154 6.00000000 4
13 -92163.179  20572.085 12.00000000 4
14 -90795.593  19111.866 12.00000000 4
15 -90796.032  19722.744 12.00000000 4
16 -91788.285  20089.386 6.00000000 4
17 -92162.564  20571.296 12.00000000 1
```

Figure 4.5: Definition of Node IDs, X, Y, Z Coordinates and Zone Numbers in Input

In the fourth part, it consists of element connectivity. In other words, it shows which elements are attached to which nodes. It also gives the relevant zones and the element lengths. It is shown in Figure 4.6.

```
LINES
id connectivity zone length
1 6 15 3 610.00000000
2 8 9  3 914.00000000
3 9 10  3 760.00000000
4 10 13  3 610.00000000
5 14 6  4 100.00000000
6 11 12  3 457.00000000
7 11 10  3 610.00000000
8 7 11  3 914.00000000
9 6 7  3 760.00000000
10 8 11  3 610.00000000
11 10 2  3 30.00000000
12 4 16  3 61.00000000
13 5 14  3 1500.00000000
14 7 3  3 975.00000000
15 15 8  4 100.00000000
16 12 17  3 610.00000000
17 16 12  4 100.00000000
18 1 5  5 100.00000000
19 17 13 4 100.00000000
```

Figure 4.6: Definition of Element Ids, Connectivities, Zones and Lengths in Input

Fifth part is the node boundary condition attributes. In this part, the input file gives the defined nodal demand discharges. It is shown in Figure 4.7.

```
NODE-BC-ATTRIBUTES
1 40 1 0.00
2 40 1 0.00
3 40 1 0.00
4 40 1 0.00
7 39 1 0.06
9 39 1 0.11
10 39 1 0.11
12 39 1 0.06
13 39 1 0.06
```

Figure 4.7: Node Boundary Condition Attributes in Input

Sixth Part is the element boundary condition attributes. In this part, $CAEeda^{TM}$ gives the element information. If the element is a pipe, the main program gives the pipe diameter and accordingly Hazen-William head loss coefficient or Darcy-

40

Weisbach pipe roughness height according to the element attributes in input. If the element is a fitting, pipe diameter and fitting coefficient (K) are also provided. If the fitting is a contraction or an expansion, both pipe diameters, before and after the change in the area should be input. Lastly, if the element is a pump, then the cut of head (COH) and Pump Head-Discharge graph's function constants should be provided. Hazen-William head loss modeling is provided in Figure 4.8.

```
LINE-BC-ATTRIBUTES
1 35 2 0.35000000 100.00000000
2 35 2 0.35000000 100.00000000
3 35 2 0.35000000 100.00000000
4 35 2 0.35000000 100.00000000
5 36 2 0.40000000 5.00000000
6 35 2 0.30000000 100.00000000
7 35 2 0.35000000 100.00000000
8 35 2 0.35000000 100.00000000
9 35 2 0.35000000 100.00000000
10 35 2 0.35000000 100.00000000
11 35 2 0.20000000 100.00000000
12 35 2 0.15000000 100.00000000
13 35 2 0.40000000 100.00000000
14 35 2 0.30000000 100.00000000
15 36 2 0.35000000 8.00000000
16 35 2 0.35000000 100.00000000
17 36 2 0.15000000 10.00000000
18 38 3 166.00000000 148.00000000 2.87990000
19 36 2 0.35000000 10.00000000
```

Figure 4.8: Element Boundary Condition Attributes in the Input for Hazen-William Head Loss Modeling

4.2 Functional Steps of the Program

In this section, functional steps of the program are expressed. General flow chart of the program which performs the pipe network analysis is shown in Figure 4.9.
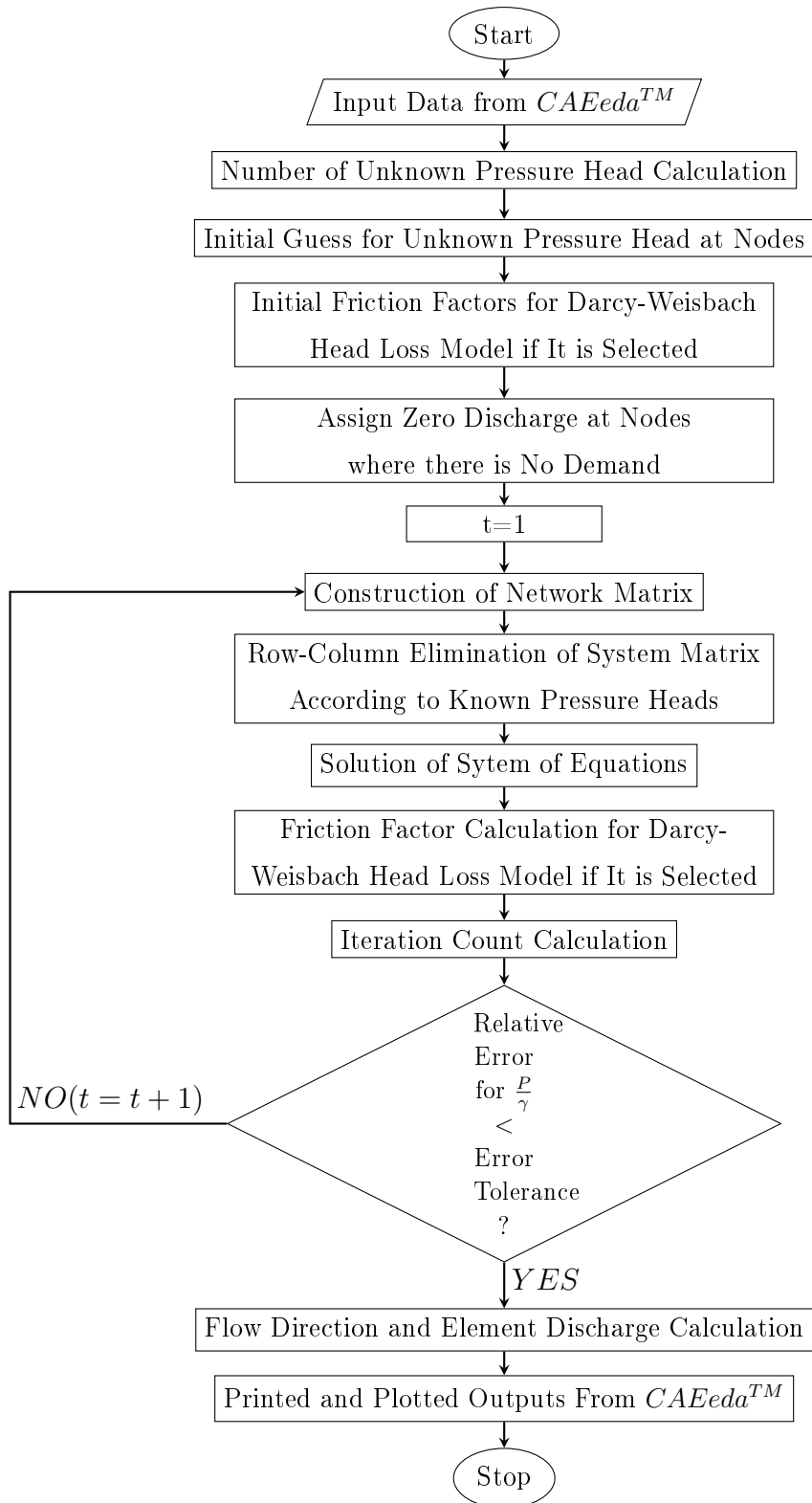
Figure 4.9: Block Diagram of the Pipe Flow Program

Firstly, symbols and notations are defined at the beginning of the program. The graphical user interface integrated to $CAEeda^{TM}$ appears to ask project name, solution type, relative error precision, and output format shown in Figure 4.1. If the user designs the network according to Hazen-Williams head loss modeling, then he must check the Hazen-Williams box. Otherwise, he must select Darcy-Weisbach. After the selection of head loss modeling type, input file which comes from the main program opens. The program starts to read the necessary flow data in input. It reads firstly node numbers, element numbers and zone numbers, respectively. Then, the program allocates the notations which will be arrays according to the element and node number. Furthermore, it continues to read input file. It reads zones, nodes' geographical information (x, y, z coordinates), element connectivity, node boundary condition attributes, element boundary condition attributes, respectively. After reading the element boundary condition attributes, the program closes the input file and starts to calculates the necessary information with using the read data.

First of all, it calculates the element areas. Then, it finds the unknown pressure head counts. After that, it assigns a random value for the unknown pressure heads because both $\left[K \right]$ matrix and $\left[P/\gamma \right]$ vector is a function of P/γ. That is why the unknown pressure heads are assigned to the random value.

Next, if the head loss modeling is Darcy-Weisbach head loss modeling, the user decides whether to calculate friction factor by given roughness height(ϵ) or to use the decided friction factor(f) instead of roughness height in input. If the Epsilon (roughness height) is chosen, it assigns the first trial friction factors. Otherwise, it does not calculate the friction factor.

Furthermore, if the demand discharges are not defined for some of the nodes, it assigns zero value for these nodes because there is no inflow or outflow at these nodes.

After all types of data are collected, computations are performed in a loop. According to hydraulic grade lines, which are a sum of pressure heads and elevation heads, flow directions of the elements are found. Then, resistance constants are calculated. After that, system matrix and $[Q^{(e)}] - C_{ij}[\Delta_z{}^{(e)}]$ calculations are done. Accordingly, row-column elimination process is done in order to impose the pressure head boundary conditions on the system which also eliminates the

singularity of the system matrix. After row-column eliminations, the matrix $_{t+1}\left[P/\gamma\right]$ is calculated. This calculation is done either with the direct solver or the conjugate gradient solver [16] which is an option in the graphical user interface shown in Figure 4.1. If the solution is done with the direct solver, the system matrix is inverted. The code which takes the inverse of the system matrix has been taken from an open source [18].

Lastly, the relative error is controlled and the loop finishes. If the relative error is greater than the defined tolerable value given in the graphical user interface, the loop returns to the beginning and do the all steps until the relative error is less than the defined value.

After the loop finishes, it calculates the last flow directions of the elements and element discharges. If the head loss modeling is Darcy-Weisbach head loss modeling, it also calculates the final friction factors and the program ends.

4.3   The Output Generation of the Program

After entering all data, user presses the "OK" button in solver gui and pipe program starts to run. After running the pipe program, it generates two output file as shown in Figure 4.2. One of them is a data file which is read by postprocess module of $CAEeda^{TM}$ to plot flow directions on the pipe network system and graphical representation of the results. The other output of the program is a text output file which shows all calculated results on the nodes and elements.

As it is seen in Figure 4.1, the only difference between Hazen-William and Darcy-Weisbach head loss modeling is the initial friction factor and the final friction factor between them.

Furthermore, all of these selections are expressed one by one below.

When the user clicks the input data box in GUI, the program prints out the entered node and element number, nodal geographical coordinates, element connectivity, nodal demand discharge and pressure head information and element characteristics. They are shown in Figures 4.10, 4.11, 4.12, 4.13 and 4.14.

```
Node Number:      17
Element Number:   19
```

Figure 4.10: Illustration of the Node and Element Number at the Output

```
Node Coordinates
Id            X                Y               Z
1      -90124.583        17769.232        3.000
2      -91553.186        20598.066       30.000
3      -91919.857        20017.137       34.000
4      -91823.029        20047.795       34.000
5      -90125.030        17770.127        3.000
6      -90796.040        19112.761       12.000
7      -91556.034        19112.761       15.000
8      -90796.032        19723.744       12.000
9      -90796.032        20637.725       18.000
10      -91553.186        20572.085       15.000
11      -91339.514        20000.739       12.000
12      -91787.643        20090.154        6.000
13      -92163.179        20572.085       12.000
14      -90795.593        19111.866       12.000
15      -90796.032        19722.744       12.000
16      -91788.285        20089.386        6.000
17      -92162.564        20571.296       12.000
```

Figure 4.11: Illustration of the Nodal Geographical Coordinates at the Output

```
Element Connectivity
Id     Node_i    Node_j        Length
[-]      [-]       [-]            [m]
1         6        15       610.000
2         8         9       914.000
3         9        10       760.000
4        10        13       610.000
5        14         6       100.000
6        11        12       457.000
7        11        10       610.000
8         7        11       914.000
9         6         7       760.000
10         8        11       610.000
11        10         2        30.000
12         4        16        61.000
13         5        14      1500.000
14         7         3       975.000
15        15         8       100.000
16        12        17       610.000
17        16        12       100.000
18         1         5       100.000
19        17        13       100.000
```

Figure 4.12: Illustration of the Element Connectivity at the Output

```
Nodal Information
Node      Demand      Pressure
Number    Discharge     Head
Id          Qi        P/Gama
[-]       [m^3/s]       [m]
1         UNKNOWN     0.0000
2         UNKNOWN     0.0000
3         UNKNOWN     0.0000
4         UNKNOWN     0.0000
5          0.0000     UNKNOWN
6          0.0000     UNKNOWN
7         -0.0600     UNKNOWN
8          0.0000     UNKNOWN
9         -0.1100     UNKNOWN
10        -0.1100     UNKNOWN
11         0.0000     UNKNOWN
12        -0.0600     UNKNOWN
13        -0.0600     UNKNOWN
14         0.0000     UNKNOWN
15         0.0000     UNKNOWN
16         0.0000     UNKNOWN
17         0.0000     UNKNOWN
```

Figure 4.13: Illustration of the Nodal Information at the Output

Element Characteristics

Id [-]	Types [-]	Nodes i [-]	Nodes j [-]	Diameter D [m]	H-W Coeff [-]	Fitting Coeff. Km [-]	Pump Characteristics hp=COH-aQ^b COH [m]	a [-]	b [-]	Contraction/ Expansion D1 [m]	D2 [m]
1	PIPE	6	15	0.350	100.00	-	-	-	-	-	-
2	PIPE	8	9	0.350	100.00	-	-	-	-	-	-
3	PIPE	9	10	0.350	100.00	-	-	-	-	-	-
4	PIPE	10	13	0.350	100.00	-	-	-	-	-	-
5	FITTING	14	6	0.400	-	5.00	-	-	-	-	-
6	PIPE	11	12	0.300	100.00	-	-	-	-	-	-
7	PIPE	11	10	0.350	100.00	-	-	-	-	-	-
8	PIPE	7	11	0.350	100.00	-	-	-	-	-	-
9	PIPE	6	7	0.350	100.00	-	-	-	-	-	-
10	PIPE	8	11	0.350	100.00	-	-	-	-	-	-
11	PIPE	10	2	0.200	100.00	-	-	-	-	-	-
12	PIPE	4	16	0.150	100.00	-	-	-	-	-	-
13	PIPE	5	14	0.400	100.00	-	-	-	-	-	-
14	PIPE	7	3	0.300	100.00	-	-	-	-	-	-
15	FITTING	15	8	0.350	-	8.00	-	-	-	-	-
16	PIPE	12	17	0.350	100.00	-	-	-	-	-	-
17	FITTING	16	12	0.150	-	10.00	-	-	-	-	-
18	PUMP	1	5	-	-	-	166.00	148.00	2.88	-	-
19	FITTING	17	13	0.350	-	10.00	-	-	-	-	-

Figure 4.14: Illustration of the Element Information at the Output

When the user clicks the Element Area box in the GUI, the program prints out the areas of the elements. They are shown in Figure 4.15. If the element is contraction or expansion, then the $D2$ and accordingly $A2$ is calculated.

```
Element Area
Element    D1      D2 |   A1       A2
Number    [m]     [m] |  [m^2]    [m^2]
  1      0.350     -  |  0.096     -
  2      0.350     -  |  0.096     -
  3      0.350     -  |  0.096     -
  4      0.350     -  |  0.096     -
  5      0.400     -  |  0.126     -
  6      0.300     -  |  0.071     -
  7      0.350     -  |  0.096     -
  8      0.350     -  |  0.096     -
  9      0.350     -  |  0.096     -
 10      0.350     -  |  0.096     -
 11      0.200     -  |  0.031     -
 12      0.150     -  |  0.018     -
 13      0.400     -  |  0.126     -
 14      0.300     -  |  0.071     -
 15      0.350     -  |  0.096     -
 16      0.350     -  |  0.096     -
 17      0.150     -  |  0.018     -
 18       -        -  |   -        -
 19      0.350     -  |  0.096     -
```

Figure 4.15: Illustration of the Element Areas at the Output

If the user clicks the Iteration Count box in the GUI, the program prints out the number of iteration steps shown in Figure 4.16.

```
Count of Iteration Steps:        52
```

Figure 4.16: Illustration of the Iteration Counts at the Output

When the user clicks the Pressure Head box or the Demand Discharge box in the GUI, the program prints out final pressure heads or final demand discharges at nodes. They are shown in Figures 4.17 and 4.18, respectively.

48

```
Pressure Head Results
Id        P/Gamma
[-]         [m]
 1         0.000
 2         0.000
 3         0.000
 4         0.000
 5       143.913
 6        49.816
 7        26.239
 8        28.320
 9        13.322
10        15.778
11        24.071
12        25.941
13        18.768
14        54.123
15        31.432
16        26.791
17        18.936
```

Figure 4.17: Illustration of the Pressure Heads at the Output

```
Demand Discharge Results
Id          Qi
[-]       [m^3/s]
 1        0.51658
 2       -0.05625
 3       -0.08316
 4        0.02283
 5        0.00000
 6        0.00000
 7       -0.06000
 8        0.00000
 9       -0.11000
10       -0.11000
11        0.00000
12       -0.06000
13       -0.06000
14        0.00000
15        0.00000
16        0.00000
17        0.00000
```

Figure 4.18: Illustration of the Demand Discharges at the Output

If the user wants to know only the flow direction and clicks the relevant box in the GUI, the program prints out final flow directions of the elements. It is shown in Figure 4.19.

```
   Flow Direction(i -> j)
    Element
Id          i     ->      j
 1          6     ->     15
 2          8     ->      9
 3          9     ->     10
 4         10     ->     13
 5         14     ->      6
 6         11     ->     12
 7         11     ->     10
 8          7     ->     11
 9          6     ->      7
10          8     ->     11
11         10     ->      2
12          4     ->     16
13          5     ->     14
14          7     ->      3
15         15     ->      8
16         12     ->     17
17         16     ->     12
18          1     ->      5
19         17     ->     13
```

Figure 4.19: Illustration of the Flow Directions at the Output

When the user wants to know only the element discharges or HGL elevations and clicks the relevant box in the GUI, the program prints out final element discharges and hydraulic grade line levels, respectively. They are illustrated in Figures 4.20 and 4.21.

```
Element Discharge Results
Id         Qij
[-]       [m^3/s]
 1        0.2658
 2        0.1453
 3        0.0353
 4        0.0047
 5        0.5166
 6        0.0925
 7        0.1357
 8        0.1077
 9        0.2508
10        0.1205
11        0.0563
12        0.0228
13        0.5166
14        0.0832
15        0.2658
16        0.0553
17        0.0228
18        0.5166
19        0.0553
```

Figure 4.20: Illustration of the Element Discharges at the Output

```
Hydraulic Grade Line Level Results
 Id    P/Gamma+z
 [-]        [m]
  1      15.000
  2      61.000
  3     192.147
  4     155.639
  5     132.590
  6     126.432
  7     122.173
  8     122.615
  9     129.739
 10     123.810
 11     136.465
 12     135.919
 13     133.023
 14     128.347
 15     122.152
 16     119.366
 17     159.958
```

Figure 4.21: Illustration of Hydraulic Grade Line Level at the Output

CHAPTER 5

CASE STUDIES

In this chapter, five test case problems will be solved by the program developed in the study. Problems and their solutions have been taken from the reference book [19]. The reference book gives the results of test case problems 4 and 5 as an EPANET output. The results of the present program which were calculated in both LU Decomposition method and Conjugate Gradient method will be compared to those obtained from the textbook.

Network symbols of the free-body diagram of the problems are shown in Figure 5.1.

■	RESERVOIR NODE SYMBOL
●	DEMAND NODE SYMBOL
1	NODE NUMBER SYMBOL
①	ELEMENT NUMBER SYMBOL
0.11m³/s	DEMAND DISCHARGE SYMBOL
⋈	VALVE SYMBOL
℗	PUMP SYMBOL

Figure 5.1: Definition of Network Symbols

5.1 Test Case Problems

Test Case 1. *For the system shown in Figure 5.2, determine water flow distribution and piezometric head at the junction. Assume constant friction factors. The pump characteristic curve is $H_P = a - bQ^2$, where $a = 20m$ and $b = 30s^2/m^5$. The reservoir elevation heads, z_1, z_2 and z_3 are $10m$, $20m$ and $18m$, respectively. Table 5.1 shows the element parameters.*
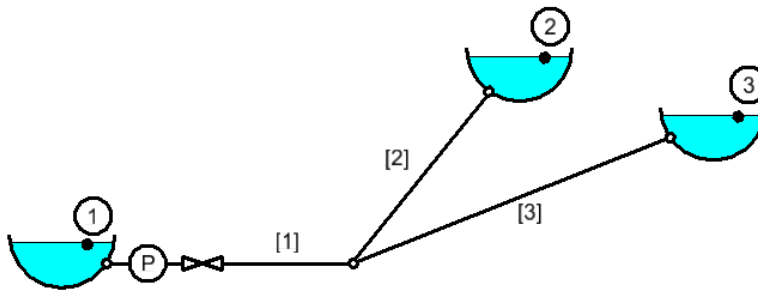

Figure 5.2: Network of Test Case 1 [19]

Table 5.1: Element Parameters of Test Case 1

Pipe	L (m)	D (cm)	f	$\sum K$
1	30	24	0.020	2
2	60	20	0.015	0
3	90	16	0.025	0

For this problem, the free-body diagram is shown in Figure 5.3. As it is seen from Figure 5.3, there are 6 nodes, 5 elements. Elements are composed of 1 pump, 1 valve and 3 pipes. There are also 3 reservoirs as nodal parameters. Element Characteristics of the system and node parameters are shown in Table 5.2 and 5.3, respectively. Element discharges are shown in Table 5.4. As it is seen at the tables, the program results are compared with the results of the book [19]. The relative errors among the results are almost none. Therefore, it is shown that the program solves this problem correctly.
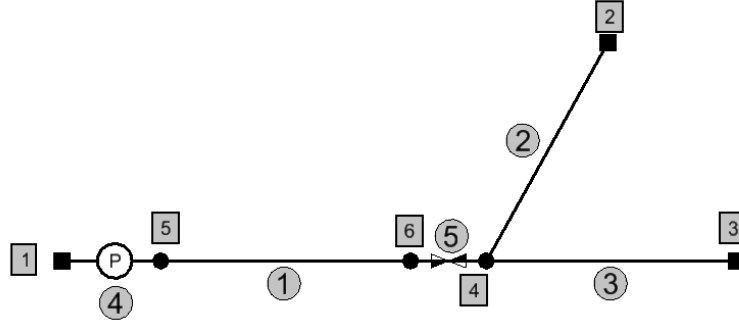
54

Figure 5.3: Free-Body Diagram of Test Case 1

Table 5.2: Element Characteristics of Test Case 1

Elem. Num.	Elem. Type	i	j	L (m)	D (m)	Friction Factor	Fitting Coeff.	Pump Parameters		
						f	K	COH	a	b
1	Pipe	5	6	30	0.24	0.020	-	-	-	-
2	Pipe	4	2	60	0.20	0.015	-	-	-	-
3	Pipe	4	3	90	0.16	0.025	-	-	-	-
4	Pump	1	5	-	-	-	-	20	30	2
5	Fitting	6	4	-	0.24	-	2.00	-	-	-

Table 5.3: Node Parameters of Test Case 1

Node Number	Pressure Head(P/γ) (m)	Demand Discharge(Q) (m^3/s)	Elevation $(Z)(m)$
1	0.00	Unknown	10
2	0.00	Unknown	20
3	0.00	Unknown	18
4	Unknown	0.00	0
5	Unknown	0.00	0
6	Unknown	0.00	0

Table 5.4: Element Discharge Comparison of Test Case 1

Element Number	Element Type	Flow Direction		Element Discharge (m^3/s)		Relative Error (%)
		i	j	Computed	Reference	
1	Pipe	5	6	0.1981	0.2000	0.95
2	Pipe	4	2	0.1380	0.1400	1.43
3	Pipe	4	3	0.0602	0.0600	-0.33
4	Pump	1	5	0.1981	-	-
5	Fitting	6	4	0.1981	-	-

Test Case 2. *Determine the flow distribution of water in the system shown in Figure 5.4. The equivalent roughness height for all elements is* 0.1mm. *Table 5.5 shows the element parameters.*
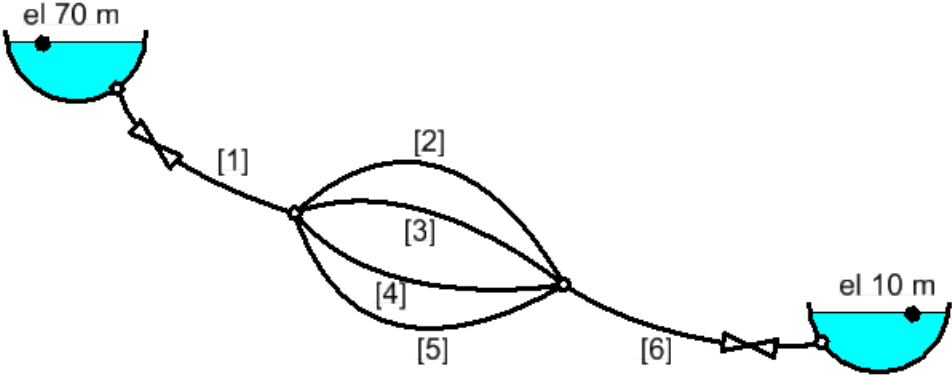
Figure 5.4: Network of Test Case 2 [19]

Table 5.5: Element Parameters of Test Case 2

Pipe	L (m)	D (mm)	$\sum K$
1	1000	200	3
2	200	25	0
3	250	25	0
4	340	30	2
5	420	40	0
6	500	175	5

For this problem, the free-body diagram is shown in Figure 5.5. As it is seen from Figure 5.5, there are 7 nodes, 9 elements. Elements are composed of 3 valves and 6 pipes. There are also 2 reservoirs as a nodal parameter.

Element characteristics of the system and node parameters are shown in Table 5.6 and 5.7, respectively. Pressure heads, demand discharges and element discharges are shown in Table 5.8. As it is seen at the table, the program results are compared with the results of the reference [19]. The relative errors between the results are almost none. Therefore, it is shown that the program solves this problem correctly.
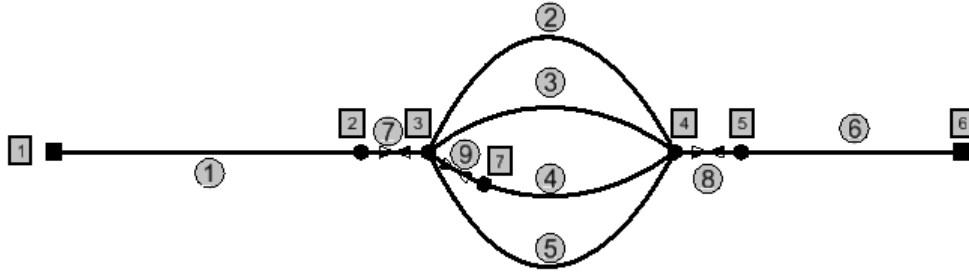
Figure 5.5: Free-Body Diagram of Test Case 2

Table 5.6: Element Characteristics of Test Case 2

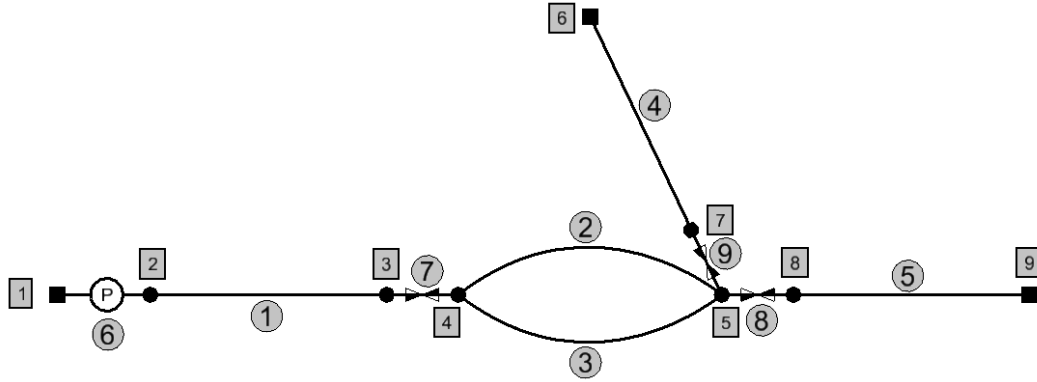| Elem. Num.	Elem. Type	i	j	L (m)	D (m)	Rough. Height	Fitting Coeff.	Pump Parameters		
						ε (mm)	K	COH	a	b
1	Pipe	1	2	1000	0.200	0.10	-	-	-	-
2	Pipe	3	4	200	0.025	0.10	-	-	-	-
3	Pipe	3	4	250	0.025	0.10	-	-	-	-
4	Pipe	7	4	340	0.030	0.10	-	-	-	-
5	Pipe	3	4	420	0.040	0.10	-	-	-	-
6	Pipe	5	6	500	0.175	0.10	-	-	-	-
7	Fitting	2	3	-	0.200	-	3.00	-	-	-
8	Fitting	4	5	-	0.175	-	5.00	-	-	-
9	Fitting	3	7	-	0.030	-	2.00	-	-	-

Table 5.7: Node Parameters of Test Case 2

Node Number	Pressure Head(P/γ) (m)	Demand Discharge(Q) $\left(m^3/s\right)$	Elevation $(Z)(m)$
1	0.00	Unknown	70
2	Unknown	0.00	0
3	Unknown	0.00	0
4	Unknown	0.00	0
5	Unknown	0.00	0
6	0.00	Unknown	10
7	Unknown	0.00	0

Table 5.8: Element Discharge Comparison of Test Case 2

Element Number	Element Type	Flow Direction		Element Discharge (m^3/s)		Relative Error (%)
		i	j	Computed	Reference	
1	Pipe	1	2	0.00590	0.00591	0.17
2	Pipe	3	4	0.00110	0.00107	-2.80
3	Pipe	3	4	0.00100	0.00095	-5.26
4	Pipe	7	4	0.00130	0.00132	1.52
5	Pipe	3	4	0.00250	0.00256	2.34
6	Pipe	5	6	0.00590	0.00591	0.17
7	Fitting	2	3	0.00590	-	-
8	Fitting	4	5	0.00590	-	-
9	Fitting	3	7	0.00130	-	-

Test Case 3. *Determine the flow distribution of water in the system shown in Figure 5.6. Assume constant friction factors, with $f = 0.02$. The head-discharge relation for the pump is $H_P = 60 - 10Q^2$, where H_P is in meters and the discharge is in cubic meters per second. Table 5.9 shows the element parameters.*
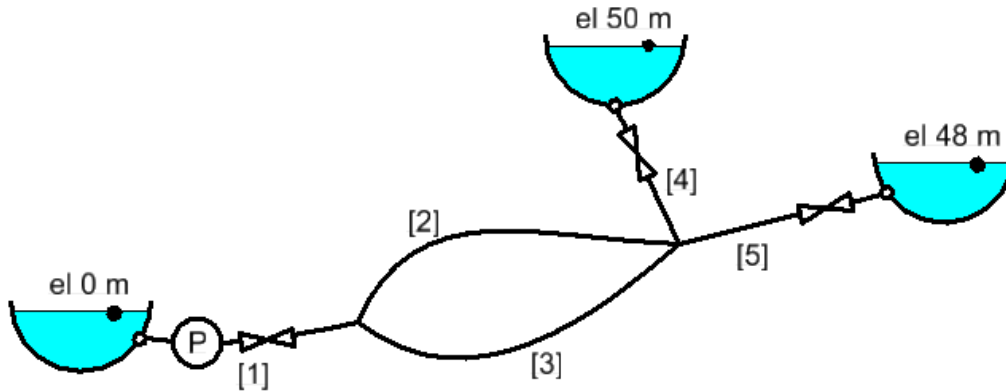
Figure 5.6: Network of Test Case 3 [19]

Table 5.9: Element Parameters of Test Case 3

Pipe	L (m)	D (mm)	$\sum K$
1	100	350	2
2	750	200	0
3	850	200	0
4	500	200	2
5	350	250	2

For this problem, the free-body diagram is shown in Figure 5.7. As it is seen from Figure 5.7, there are 9 nodes, 9 elements. Elements are composed of 1 pump, 3 valves and 5 pipes. There are also 3 reservoirs as nodal parameters. Element Characteristics of the system and node parameters are shown in Table 5.10 and 5.11, respectively. Pressure heads, demand discharges and element discharges are shown in Table 5.12. As it is seen at the table, the program results are compared with the results of the book [19]. The relative errors among the results are almost none. Therefore, it is shown that the program solves this problem correctly.
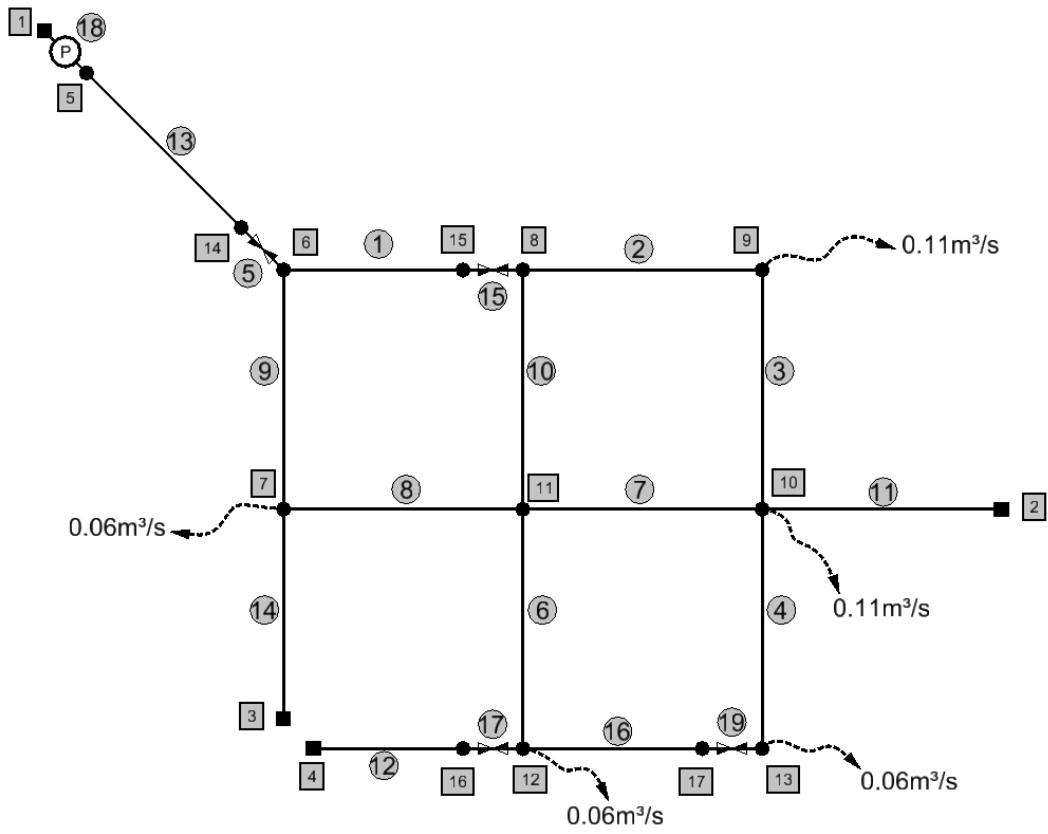
Figure 5.7: Free-Body Diagram of Test Case 3

Table 5.10: Element Characteristics of Test Case 3

Elem. Num.	Elem. Type	i	j	L (m)	D (m)	Friction Factor	Fitting Coeff.	Pump Parameters		
						f	K	COH	a	b
1	Pipe	2	3	100	0.35	0.020	-	-	-	-
2	Pipe	4	5	750	0.20	0.020	-	-	-	-
3	Pipe	4	5	850	0.20	0.020	-	-	-	-
4	Pipe	6	7	500	0.20	0.020	-	-	-	-
5	Pipe	9	8	350	0.25	0.020	-	-	-	-
6	Pump	1	2	-	-	-	-	60	10	2
7	Fitting	3	4	-	0.35	-	2.00	-	-	-
8	Fitting	5	8	-	0.25	-	2.00	-	-	-
9	Fitting	7	5	-	0.20	-	2.00	-	-	-

Table 5.11: Node Parameters of Test Case 3

Node Number	Pressure Head(P/γ) (m)	Demand Discharge(Q) (m^3/s)	Elevation (Z)(m)
1	0.00	Unknown	0
2	Unknown	0.00	0
3	Unknown	0.00	0
4	Unknown	0.00	0
5	Unknown	0.00	0
6	0.00	Unknown	50
7	Unknown	0.00	0
8	Unknown	0.00	0
9	0.00	Unknown	48

Table 5.12: Element Discharge Comparison of Test Case 3

Element Number	Element Type	Flow Direction		Element Discharge (m^3/s)		Relative Error (%)
		i	j	Computed	Reference	
1	Pipe	2	3	0.0906	0.0900	-0.67
2	Pipe	4	5	0.0467	0.0460	-1.52
3	Pipe	4	5	0.0439	0.0440	0.23
4	Pipe	7	6	0.0204	0.0200	-2.00
5	Pipe	8	9	0.0701	0.0700	-0.14
6	Pump	1	2	0.0906	-	-
7	Fitting	3	4	0.0906	-	-
8	Fitting	5	8	0.0701	-	-
9	Fitting	5	7	0.0204	-	-

Test Case 4. *Determine the flow distribution for the 14-pipe water supply system shown in Figure 5.8. The characteristic curve for the pump is represented by 3 point data located on the curve, shown in Figure 5.8. (courtesy of D. Wood):*
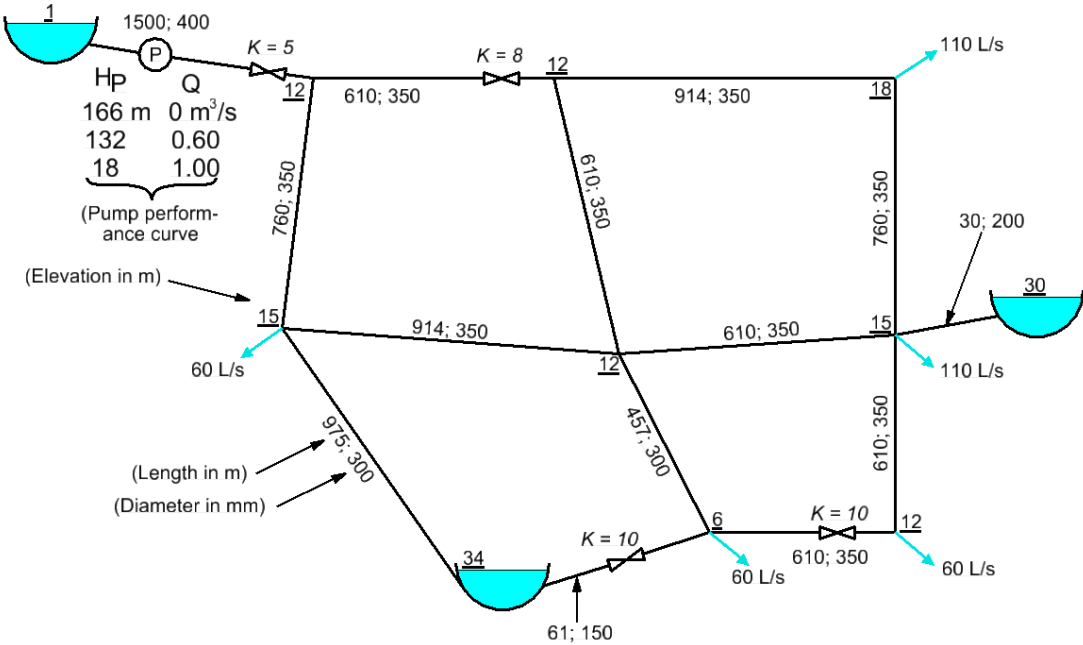
Figure 5.8: Network of Test Case 4 [19]

For this problem, the free-body diagram is shown in Figure 5.9. As it is seen from Figure 5.9, there are 17 nodes, 19 elements. Elements are composed of 1 pump, 4 valves and 14 pipes. There are also 4 reservoirs as nodal parameters. Actually, it should be 3. However, one of which is added to satisfy the connectivity of two pipes to the reservoir for FEM formulation as shown in Figure 5.9.

Element Characteristics of the system and node parameters are shown in Table 5.13 and 5.14, respectively. Pressure heads and element discharges are shown in Table 5.15 and 5.16, respectively. When the program solves the problem, it plots the flow directions on the network shown in Figure 5.10. As it is seen in the tables, the program results are compared with the results of the reference book. The relative errors between the results are almost none. Therefore, it is demonstrated that the program solves this problem satisfactorily.

Figure 5.9: Free-Body Diagram of Test Case 4
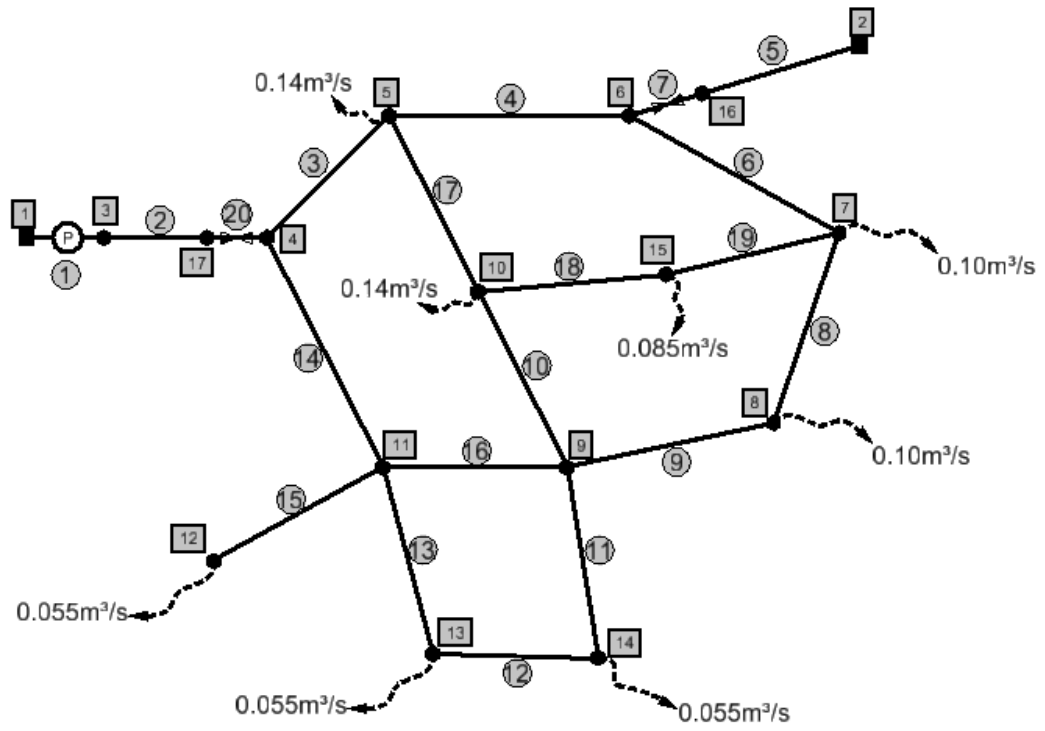
Table 5.13: Element Characteristics of Test Case 4

Element Number	Element Type	i	j	L (m)	D (m)	Pipe Coefficient	Fitting Coefficient	Pump Parameters		
						C_{HW}	K	COH	a	b
1	Pipe	6	15	610	0.35	100	-	-	-	-
2	Pipe	8	9	914	0.35	100	-	-	-	-
3	Pipe	9	10	760	0.35	100	-	-	-	-
4	Pipe	10	13	610	0.35	100	-	-	-	-
5	Fitting	14	6	-	0.40	-	5	-	-	-
6	Pipe	11	12	457	0.30	100	-	-	-	-
7	Pipe	11	10	610	0.35	100	-	-	-	-
8	Pipe	7	11	914	0.35	100	-	-	-	-
9	Pipe	6	7	760	0.35	100	-	-	-	-
10	Pipe	8	11	610	0.35	100	-	-	-	-
11	Pipe	10	2	30	0.20	100	-	-	-	-
12	Pipe	4	16	61	0.15	100	-	-	-	-
13	Pipe	5	14	1500	0.40	100	-	-	-	-
14	Pipe	7	3	975	0.30	100	-	-	-	-
15	Fitting	15	8	-	0.35	-	8	-	-	-
16	Pipe	12	17	610	0.35	100	-	-	-	-
17	Fitting	16	12	-	0.15	-	10	-	-	-
18	Pump	1	5	-	-	-	-	166	148	2.8799
19	Fitting	17	13	-	0.35	-	10	-	-	-

Table 5.14: Node Parameters of Test Case 4

Node Number	Pressure Head(P/γ) (m)	Demand Discharge(Q) (m^3/s)	Elevation (Z)(m)
1	0.00	Unknown	3
2	0.00	Unknown	30
3	0.00	Unknown	34
4	0.00	Unknown	34
5	Unknown	0.00	3
6	Unknown	0.00	12
7	Unknown	0.06	15
8	Unknown	0.00	12
9	Unknown	0.11	18
10	Unknown	0.11	15
11	Unknown	0.00	12
12	Unknown	0.06	6
13	Unknown	0.06	12
14	Unknown	0.00	12
15	Unknown	0.00	12
16	Unknown	0.00	6
17	Unknown	0.00	12

Table 5.15: Pressure Head Comparison of Test Case 4

Node Number	Pressure Head (P/γ) (m)		Relative Error (%)
	Computed	Reference	
1	0.000	0.000	Given
2	0.000	0.000	Given
3	0.000	0.000	Given
4	0.000	0.000	Given
5	143.913	143.930	0.01
6	49.816	49.820	0.01
7	26.239	26.240	0.00
8	28.320	28.320	0.00
9	13.322	13.320	-0.02
10	15.778	15.780	0.01
11	24.071	24.070	0.00
12	25.941	25.940	0.00
13	18.768	18.770	0.01
14	54.123	-	-
15	31.432	-	-
16	26.791	-	-
17	18.936	-	-

Table 5.16: Element Discharge Comparison of Test Case 4

Element Number	Element Type	Flow Direction		Element Discharge (m^3/s)		Relative Error (%)
		i	j	Computed	Reference	
1	Pipe	6	15	0.26580	0.26567	-0.05
2	Pipe	8	9	0.14530	0.14521	-0.06
3	Pipe	9	10	0.03530	0.03521	-0.26
4	Pipe	10	13	0.00470	0.00472	0.42
5	Fitting	14	6	0.51660	-	-
6	Pipe	11	12	0.09250	0.09245	-0.05
7	Pipe	11	10	0.13570	0.13563	-0.05
8	Pipe	7	11	0.10770	0.10762	-0.07
9	Pipe	6	7	0.25080	0.25073	-0.03
10	Pipe	8	11	0.12050	0.12046	-0.03
11	Pipe	10	2	0.05630	0.05612	-0.32
12	Pipe	4	16	0.02280	0.02283	0.13
13	Pipe	5	14	0.51660	0.51640	-0.04
14	Pipe	7	3	0.08320	0.08311	-0.11
15	Fitting	15	8	0.26580	-	-
16	Pipe	12	17	0.05530	0.05528	-0.04
17	Fitting	16	12	0.02280	-	-
18	Pump	1	5	0.51660	0.51640	-0.04
19	Fitting	17	13	0.05530	-	-
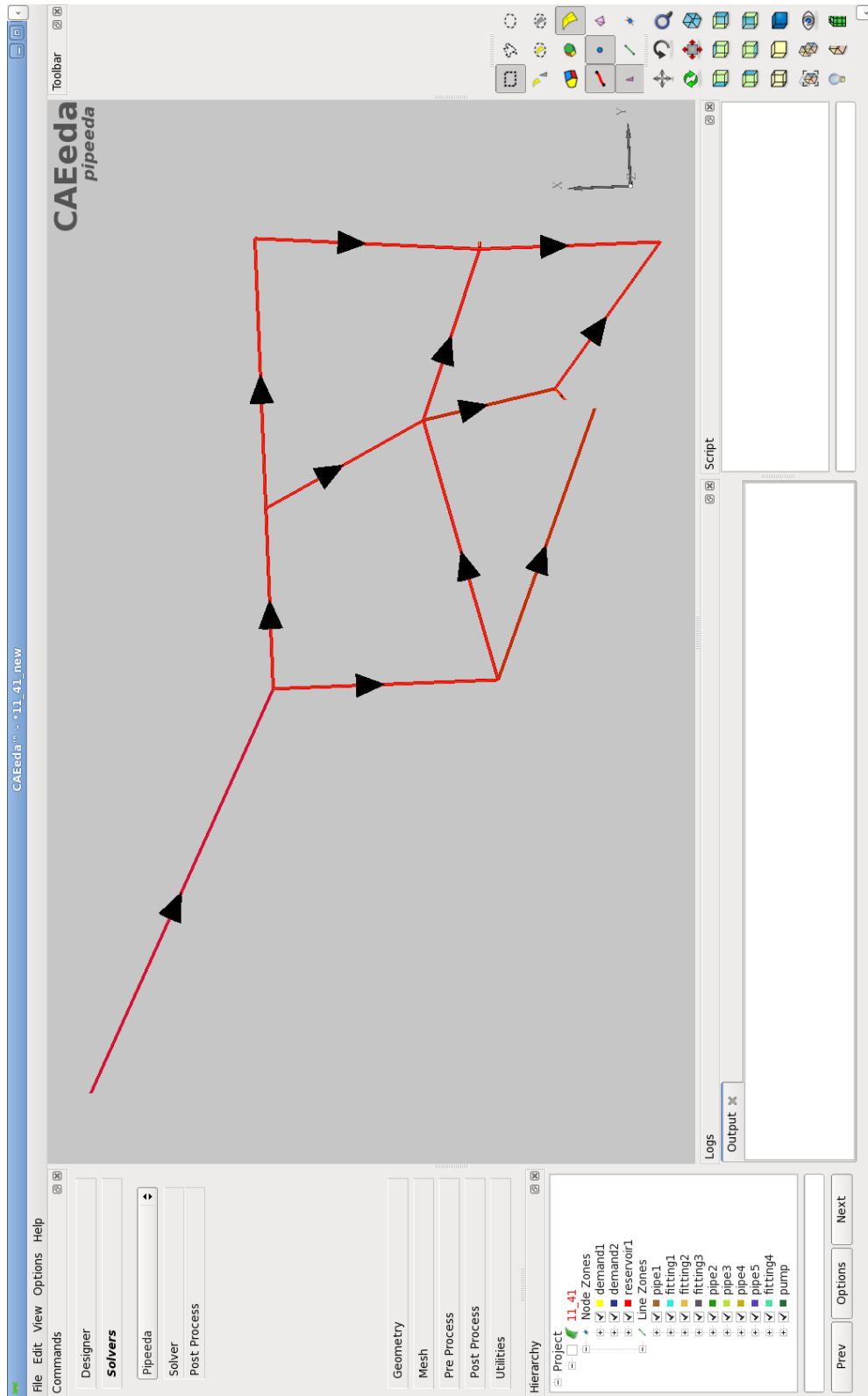
Figure 5.10: Vector View of Flow Directions of Test Case 4 from $CAEeda^{TM}$

Test Case 5. *For the piping system shown in Figure 5.11, determine the flow distribution and piozemetric heads at the junctions. Friction losses are based on the Darcy-Weisbach relation with an absolute roughness of* 0.15mm *for all pipes and a kinematic viscosity of* $10^{-6}m^2/s$.
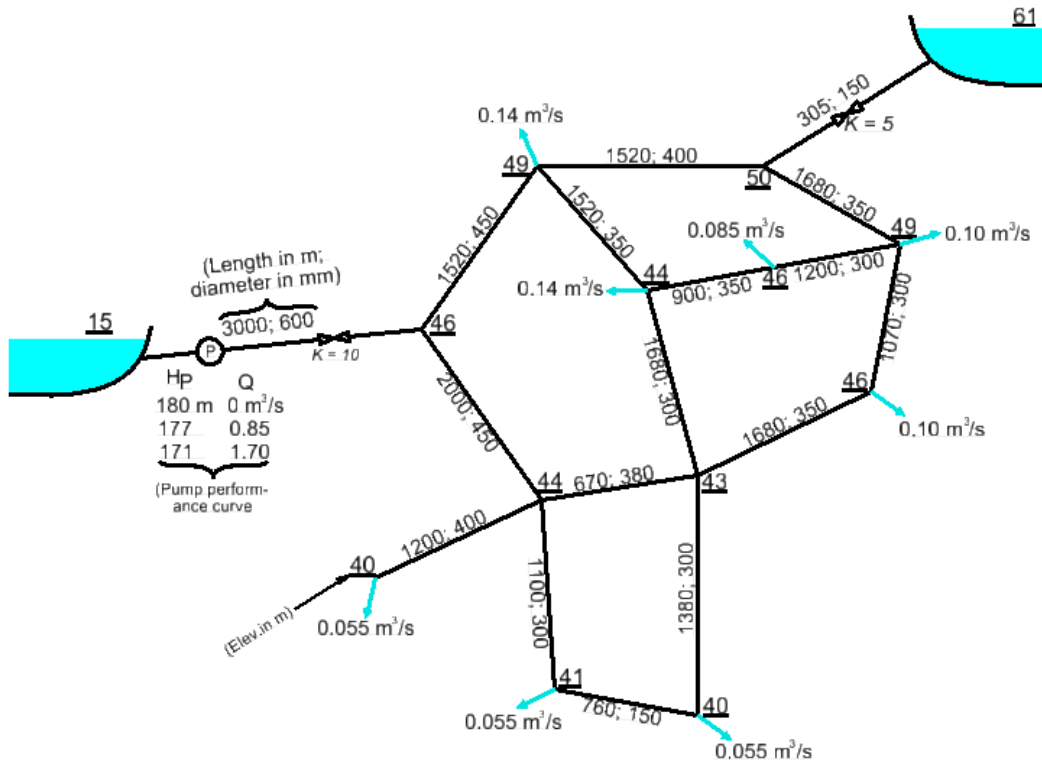
Figure 5.11: Network of Test Case 5 [19]

For this problem, the free-body diagram is shown in Figure 5.12. As it is seen from Figure 5.12, there are 17 nodes, 20 elements. Elements are composed of 1 pump, 2 valve and 17 pipes. There are also 2 reservoirs as nodal parameters. Element Characteristics of the system and node parameters are shown in Table 5.17 and 5.18, respectively. Pressure heads and element discharges are shown in Table 5.19 and 5.20, respectively. When the program solves the problem, it plots the flow directions on the network as shown in Figure 5.13. As it is seen at the tables, the program results are compared with the results of the reference book. The relative errors among the results are very negligible with only one exception. There is only one relative error which is too big while comparing the computed and the reference results. This happens to be 19th element's discharge. However, continuity equations are satisfied at each node for both the computed

70

and the reference results.

Figure 5.12: Free-Body Diagram of Test Case 5

Table 5.17: Element Characteristics of Test Case 5

Element Number	Element Type	i	j	L(m)	D(m)	Roughness Height of Pipe Wall (mm) ε	Fitting Coefficient K	Pump Parameters		
								COH	a	b
1	Pump	1	3	-	-	-	-	180	3.7	1.7
2	Pipe	3	17	3000	0.60	0.15	-	-	-	-
3	Pipe	4	5	1520	0.45	0.15	-	-	-	-
4	Pipe	5	6	1520	0.40	0.15	-	-	-	-
5	Pipe	16	2	305	0.15	0.15	-	-	-	-
6	Pipe	6	7	1680	0.35	0.15	-	-	-	-
7	Fitting	6	16	-	0.15	-	5	-	-	-
8	Pipe	7	8	1070	0.30	0.15	-	-	-	-
9	Pipe	8	9	1680	0.35	0.15	-	-	-	-
10	Pipe	9	10	1680	0.30	0.15	-	-	-	-
11	Pipe	9	14	1380	0.30	0.15	-	-	-	-
12	Pipe	14	13	760	0.15	0.15	-	-	-	-
13	Pipe	13	11	1100	0.30	0.15	-	-	-	-
14	Pipe	11	4	2000	0.45	0.15	-	-	-	-
15	Pipe	11	12	1200	0.40	0.15	-	-	-	-
16	Pipe	9	11	670	0.38	0.15	-	-	-	-
17	Pipe	10	5	1520	0.35	0.15	-	-	-	-
18	Pipe	10	15	900	0.35	0.15	-	-	-	-
19	Pipe	15	7	1200	0.30	0.15	-	-	-	-
20	Fitting	17	4	-	0.60	-	10	-	-	-

Table 5.18: Node Parameters of Test Case 5

Node Number	Pressure Head(P/γ) (m)	Demand Discharge(Q) (m^3/s)	Elevation (Z)(m)
1	0.00	Unknown	15
2	0.00	Unknown	61
3	Unknown	0.000	15
4	Unknown	0.000	46
5	Unknown	0.140	49
6	Unknown	0.000	50
7	Unknown	0.100	49
8	Unknown	0.100	46
9	Unknown	0.000	43
10	Unknown	0.140	44
11	Unknown	0.000	44
12	Unknown	0.055	40
13	Unknown	0.055	41
14	Unknown	0.055	40
15	Unknown	0.085	46
16	Unknown	0.000	50
17	Unknown	0.000	46

Table 5.19: Pressure Head Comparison of Test Case 5

Node Number	Pressure Head (P/γ) (m)		Relative Error (%)
	Computed	Reference	
1	0.000	0.000	Given
2	0.000	0.000	Given
3	177.145	177.150	0.00
4	109.711	109.490	-0.20
5	83.757	83.550	-0.25
6	76.608	76.030	-0.76
7	73.440	73.640	0.27
8	76.876	77.040	0.21
9	86.947	87.000	0.06
10	80.060	80.130	0.09
11	92.632	92.560	-0.08
12	96.093	96.020	-0.08
13	92.213	92.120	-0.10
14	88.573	88.610	0.04
15	76.419	76.590	0.22
16	69.501	-	-
17	114.032	-	-

Table 5.20: Element Discharge Comparison of Test Case 5

Element Number	Element Type	Flow Direction		Element Discharge (m^3/s)		Relative Error (%)
		i	j	Computed	Reference	
1	Pump	1	3	0.82330	0.82311	-0.02
2	Pipe	3	17	0.82330	0.82311	-0.02
3	Pipe	4	5	0.45910	0.46026	0.25
4	Pipe	5	6	0.17330	0.17763	2.44
5	Pipe	16	2	0.09330	0.09311	-0.20
6	Pipe	6	7	0.08000	0.08452	5.35
7	Fitting	6	16	0.09330	-	-
8	Pipe	8	7	0.02430	0.02287	-6.25
9	Pipe	9	8	0.12430	0.12287	-1.16
10	Pipe	9	10	0.07490	0.07498	0.11
11	Pipe	9	14	0.03910	0.03919	0.23
12	Pipe	13	14	0.01590	0.01581	-0.57
13	Pipe	11	13	0.07090	0.07081	-0.13
14	Pipe	4	11	0.36430	0.36285	-0.40
15	Pipe	11	12	0.05500	0.05500	0.00
16	Pipe	11	9	0.23840	0.23704	-0.57
17	Pipe	5	10	0.14570	0.14263	-2.15
18	Pipe	10	15	0.08070	0.07761	-3.98
19	Pipe	7	15	0.00430	0.00739	41.81
20	Fitting	17	4	0.82330	-	-
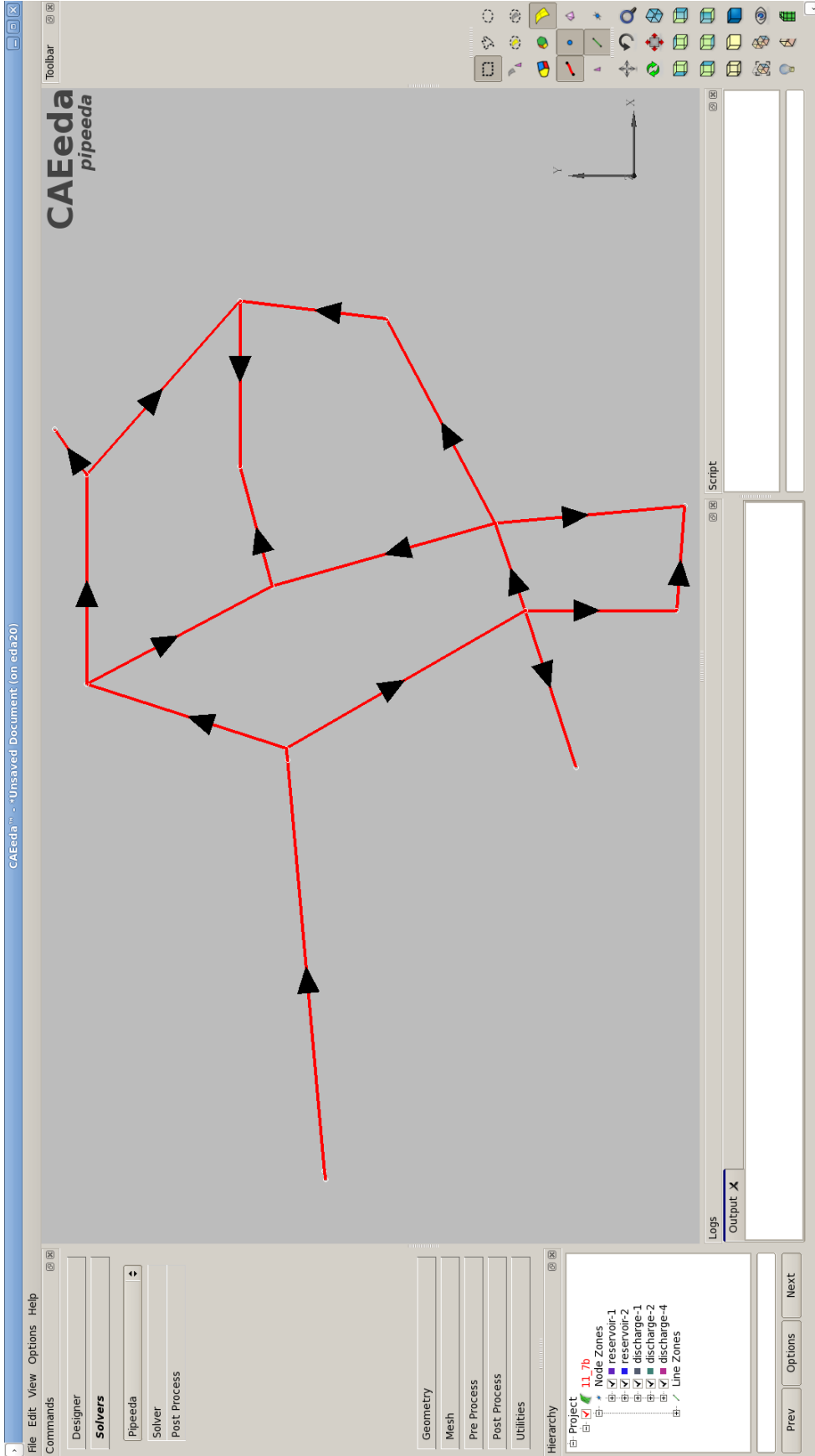
Figure 5.13: Vector View of Flow Directions of Test Case 5 from *CAEeda*^{TM}

CHAPTER 6

CONCLUSIONS AND RECOMMENDATIONS

6.1 Summary and Conclusions

In this thesis, a pipe network solution program is developed by using the Finite Element Method to run under an existing computer aided engineering software package $CAEeda^{TM}$ [1]. The program is capable of solving inflow or outflow discharges at the reservoir nodes, pressure heads at the junctions and the demand nodes and pipe element discharges in the network.

Large variety of elements, such as pipe, bend, elbow, tee, contraction, expansion, pump, etc. may be considered.

The program have been tested with several types of networks expressed in Chapter 5. The good agreement between program and reference solutions has been observed. By using geometry, pre and post process capabilities of $CAEeda^{TM}$, as a result of the program integration, complex pipe network systems can be analyzed easily. By these ways, it may be used as a promising tool for pipe network analysis.

6.2 Recommendations

This program may be thought as a prototype solver for pipe networks. Some methods may also be implemented to the program in the further studies as mentioned belows:

- Pipe network optimizations

- Solution of unsteady-state (water hammer) pipe network analysis

- Solution of pipe network analysis for unknown resistance constant

- Inclusion of the choice for pump characteristics curve data (Currently, 3 point data form is used)

REFERENCES

[1] CAEeda. `http://www.caeeda.com`. [accessed September-2016].

[2] WaterCAD-Bentley. `https://www.bentley.com/en/products/product-line/hydraulics-and-hydrology-software/watercad`. [accessed September-2016].

[3] AFT Piping Software. `http://www.aft.com/products?gclid=CIHcs8Sjic8CFUI_GwodpIMHKQ`. [accessed September-2016].

[4] EPANET. `https://www.epa.gov/water-research/epanet`. [accessed September-2016].

[5] R. Mohtar, V. Bralts, and W. Shayya. A finite element model for the analysis and optimization of pipe networks. *Transactions of the ASAE (USA)*, 1991.

[6] P. R. Bhave. Analysis of flow in water distribution networks. In *Analysis of flow in water distribution networks*. Technomic Publishing, 1991.

[7] H. Cross. Analysis of flow in networks of conduits or conductors. *University of Illinois. Engineering Experiment Station. Bulletin; no. 286*, 1936.

[8] R. J. CORNISH. The analysis of flow in networks of pipes.(includes plates and appendices). *Journal of the Institution of Civil Engineers*, 13(2):147–154, 1939.

[9] M. S. McIlroy. Pipeline network flow analysis using ordinary algebra. *Journal (American Water Works Association)*, 41(5):422–428, 1949.

[10] T. A. Marlow, R. L. Hardison, H. Jacobson, and G. E. Biggs. Improved design of fluid networks with computers. *Journal of the Hydraulics Division*, 92(4):43–61, 1966.

[11] J. Muir. Discussion of" improved design of fluid networks with computers," by ta marlow et al. *Journal of Hydraulic Division, ASCE*, 93(HY2):88–90, 1967.

[12] D. J. Wood and C. O. Charles. Hydraulic network analysis using linear theory. *Journal of the Hydraulics division*, 98(7):1157–1170, 1972.

[13] D. F. Young, B. R. Munson, T. H. Okiishi, and W. W. Huebsch. *A brief introduction to fluid mechanics*. John Wiley & Sons, 2007.

[14] P. K. Swamee and A. K. Sharma. *Design of water supply pipe networks.* John Wiley & Sons, 2008.

[15] J. N. Reddy. *An introduction to the finite element method,* volume 2. McGraw-Hill New York, 1993.

[16] Y.-H. Dai and Y. Yuan. A nonlinear conjugate gradient method with a strong global convergence property. *SIAM Journal on Optimization,* 10(1):177–182, 1999.

[17] Qt. `https://www.qt.io/product/`. [accessed September-2016].

[18] Computing Inverse matrix. `http://ww2.odu.edu/~agodunov/computing/programs/book2/Ch06/Inverse.f90`. [accessed December-2015].

[19] M. C. Potter and D. C. Wiggert. *Mechanics of Fluids Third Edition.* Bill Stenquist, 2001.

APPENDIX A

CONTINUITY CHECK FOR EACH NODE FOR TEST CASE PROBLEMS

In this appendix, continuity checks of the test case problems at each node is performed in order to verify the correctness of the solutions. Hand Calculations are used here, but the same checks is made by the program by back substituting the calculated pressure heads at the nodes to the system of linear equations.

To satisfy the continuity equation, total inflow must be equal to the total outflow at each node. This is shown below.

$$\sum Q_{inflow} = \sum Q_{outflow} \tag{A.1}$$

or

$$\sum Q_{inflow} - \sum Q_{outflow} = 0 \tag{A.2}$$

A.1   Continuity Check for Each Node for Test Case 1
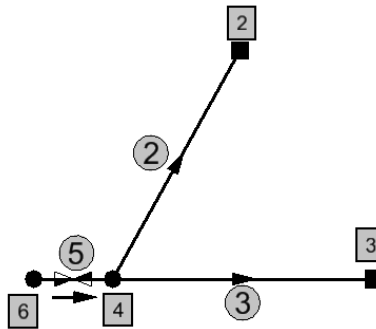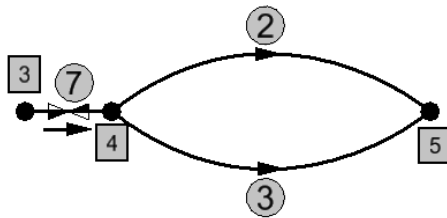

Figure A.1: Continuity for Node 4 in Test Case 1

Continuity equation for node 4 is as follows.

$$\sum Q_{inflow} = Q^{(5)}_{6 \ to \ 4}$$

$$= 0.1981 \frac{m^3}{s}$$

$$\sum Q_{outflow} = Q^{(2)}_{5 \ to \ 2} + Q^{(3)}_{4 \ to \ 3}$$

$$= 0.1380 + 0.0602$$

$$= 0.1982 \frac{m^3}{s}$$

$$\sum Q_{inflow} - \sum Q_{outflow} = Q^{(5)}_{6 \ to \ 4} - Q^{(2)}_{5 \ to \ 2} - Q^{(3)}_{4 \ to \ 3}$$

$$= 0.1981 - 0.1982$$

$$= -0.0001 \frac{m^3}{s}$$

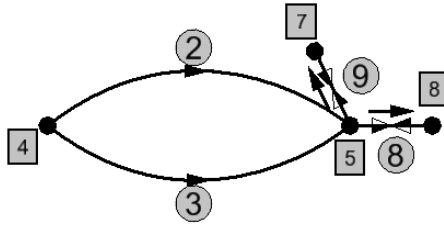Error is only $0.0001 m^3/s$. Continuity equation is satisfied at the 4th node.
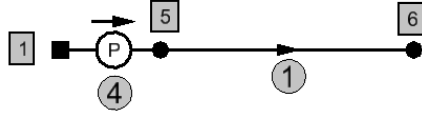
Figure A.2: Continuity for Node 5 in Test Case 1

Continuity equation for node 5 is as follows.

$$\sum Q_{inflow} = Q^{(4)}_{1 \ to \ 5}$$

$$= 0.1981 \frac{m^3}{s}$$

$$\sum Q_{outflow} = Q^{(1)}_{5 \ to \ 6}$$

$$= 0.1981 \frac{m^3}{s}$$

$$\sum Q_{inflow} - \sum Q_{outflow} = Q^{(4)}_{1 \ to \ 5} - Q^{(1)}_{5 \ to \ 6}$$

$$= 0.1981 - 0.1981$$

$$= 0.0000 \frac{m^3}{s}$$

82

Continuity equation is satisfied at the 5th node.
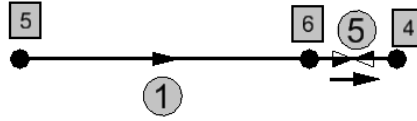
Figure A.3: Continuity for Node 6 in Test Case 1

Continuity equation for node 6 is as follows.

$$\sum Q_{inflow} = Q_{5\ to\ 6}^{(1)}$$
$$= 0.1981\frac{m^3}{s}$$

$$\sum Q_{outflow} = Q_{6\ to\ 4}^{(5)}$$
$$= 0.1981\frac{m^3}{s}$$

$$\sum Q_{inflow} - \sum Q_{outflow} = Q_{5\ to\ 6}^{(1)} - Q_{6\ to\ 4}^{(5)}$$
$$= 0.1981 - 0.1981$$
$$= 0.0000\frac{m^3}{s}$$

Continuity equation is satisfied at the 6th node.

A.2   Continuity Check for Each Node for Test Case 2
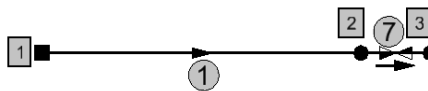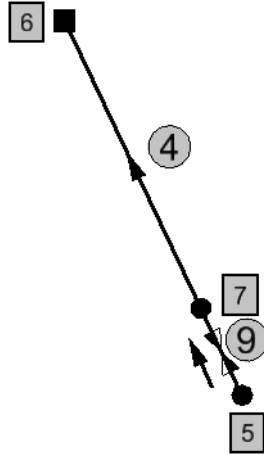

Figure A.4: Continuity for Node 2 in Test Case 2

Continuity equation for node 2 is as follows.

$$\sum Q_{inflow} = Q^{(1)}_{1\ to\ 2}$$

$$= 0.0059\frac{m^3}{s}$$

$$\sum Q_{outflow} = Q^{(7)}_{2\ to\ 3}$$

$$= 0.0059\frac{m^3}{s}$$

$$\sum Q_{inflow} - \sum Q_{outflow} = Q^{(1)}_{1\ to\ 2} - Q^{(7)}_{2\ to\ 3}$$

$$= 0.0059 - 0.0059$$

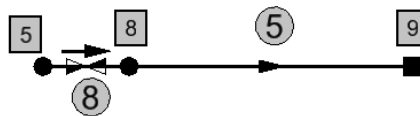$$= 0.0000\frac{m^3}{s}$$

Continuity equation is satisfied at the 2nd node.
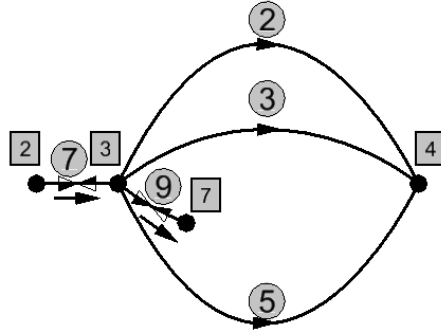
Figure A.5: Continuity for Node 3 in Test Case 2

Continuity equation for node 3 is as follows.

$$\sum Q_{inflow} = Q^{(7)}_{2\ to\ 3}$$

$$= 0.0059\frac{m^3}{s}$$

$$\sum Q_{outflow} = Q^{(2)}_{3\ to\ 4} + Q^{(3)}_{3\ to\ 4} + Q^{(9)}_{3\ to\ 7} + Q^{(5)}_{3\ to\ 4}$$

$$= 0.0011 + 0.0010 + 0.0013 + 0.0025$$

$$= 0.0059\frac{m^3}{s}$$

$$\sum Q_{inflow} - \sum Q_{outflow} = Q^{(7)}_{2\ to\ 3} - Q^{(2)}_{3\ to\ 4} - Q^{(3)}_{3\ to\ 4} - Q^{(9)}_{3\ to\ 7} - Q^{(5)}_{3\ to\ 4}$$

$$= 0.0059 - 0.0059$$

$$= 0.0000 \frac{m^3}{s}$$

Continuity equation is satisfied at the 3rd node.

Figure A.6: Continuity for Node 4 in Test Case 2

Continuity equation for node 4 is as follows.

$$\sum Q_{inflow} = Q^{(2)}_{3\ to\ 4} + Q^{(3)}_{3\ to\ 4} + Q^{(4)}_{7\ to\ 4} + Q^{(5)}_{3\ to\ 4}$$

$$= 0.0011 + 0.0010 + 0.0013 + 0.0025$$

$$= 0.0059 \frac{m^3}{s}$$

$$\sum Q_{outflow} = Q^{(8)}_{4\ to\ 5}$$

$$= 0.0059 \frac{m^3}{s}$$

$$\sum Q_{inflow} - \sum Q_{outflow} = Q^{(2)}_{3\ to\ 4} + Q^{(3)}_{3\ to\ 4} + Q^{(4)}_{7\ to\ 4} + Q^{(5)}_{3\ to\ 4} - Q^{(8)}_{4\ to\ 5}$$

$$= 0.0059 - 0.0059$$

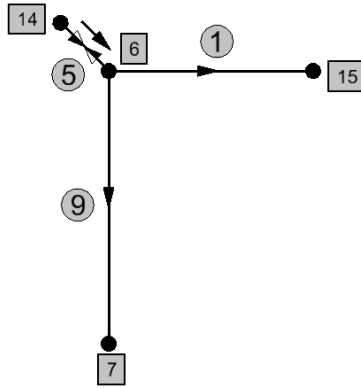$$= 0.0000 \frac{m^3}{s}$$

Continuity equation is satisfied at the 4th node.

Figure A.7: Continuity for Node 5 in Test Case 2

Continuity equation for node 5 is as follows.

$$\sum Q_{inflow} = Q^{(8)}_{4 \ to \ 5}$$
$$= 0.0059 \frac{m^3}{s}$$

$$\sum Q_{outflow} = Q^{(6)}_{5 \ to \ 6}$$
$$= 0.0059 \frac{m^3}{s}$$

$$\sum Q_{inflow} - \sum Q_{outflow} = Q^{(8)}_{4 \ to \ 5} - Q^{(6)}_{5 \ to \ 6}$$
$$= 0.0059 - 0.0059$$
$$= 0.0000 \frac{m^3}{s}$$

Continuity equation is satisfied at the 5th node.
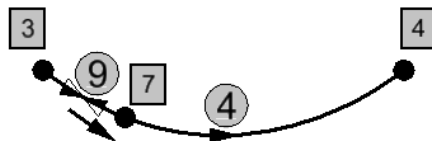
Figure A.8: Continuity for Node 7 in Test Case 2

Continuity equation for node 7 is as follows.

$$\sum Q_{inflow} = Q^{(9)}_{3 \ to \ 7}$$
$$= 0.0013 \frac{m^3}{s}$$

$$\sum Q_{outflow} = Q^{(4)}_{7 \text{ to } 4}$$

$$= 0.0013 \frac{m^3}{s}$$

$$\sum Q_{inflow} - \sum Q_{outflow} = Q^{(9)}_{3 \text{ to } 7} - Q^{(4)}_{7 \text{ to } 4}$$

$$= 0.0013 - 0.0013$$

$$= 0.0000 \frac{m^3}{s}$$

Continuity equation is satisfied at the 7th node.

A.3   Continuity Check for Each Node for Test Case 3
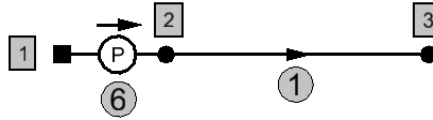
Figure A.9: Continuity for Node 2 in Test Case 3

Continuity equation for node 2 is as follows.

$$\sum Q_{inflow} = Q^{(6)}_{1 \text{ to } 2}$$

$$= 0.0906 \frac{m^3}{s}$$

$$\sum Q_{outflow} = Q^{(1)}_{2 \text{ to } 3}$$

$$= 0.0906 \frac{m^3}{s}$$

$$\sum Q_{inflow} - \sum Q_{outflow} = Q^{(6)}_{1 \text{ to } 2} - Q^{(1)}_{2 \text{ to } 3}$$

$$= 0.0906 - 0.0906$$
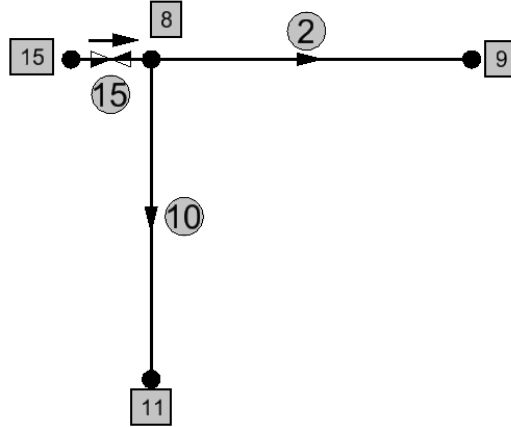
$$= 0.0000 \frac{m^3}{s}$$

Continuity equation is satisfied at the 2nd node.

Figure A.10: Continuity for Node 3 in Test Case 3

Continuity equation for node 3 is as follows.

$$\sum Q_{inflow} = Q^{(1)}_{2\ to\ 3}$$
$$= 0.0906 \frac{m^3}{s}$$

$$\sum Q_{outflow} = Q^{(7)}_{3\ to\ 4}$$
$$= 0.0906 \frac{m^3}{s}$$

$$\sum Q_{inflow} - \sum Q_{outflow} = Q^{(1)}_{2\ to\ 3} - Q^{(7)}_{3\ to\ 4}$$
$$= 0.0906 - 0.0906$$
$$= 0.0000 \frac{m^3}{s}$$

Continuity equation is satisfied at the 3rd node.

Figure A.11: Continuity for Node 4 in Test Case 3

Continuity equation for node 4 is as follows.

$$\sum Q_{inflow} = Q^{(7)}_{3\ to\ 4}$$
$$= 0.0906 \frac{m^3}{s}$$

88

$$\sum Q_{outflow} = Q^{(2)}_{4 \, to \, 5} + Q^{(3)}_{4 \, to \, 5}$$

$$= 0.0467 + 0.0439$$

$$= 0.0906 \frac{m^3}{s}$$

$$\sum Q_{inflow} - \sum Q_{outflow} = Q^{(7)}_{3 \, to \, 4} - Q^{(2)}_{4 \, to \, 5} - Q^{(3)}_{4 \, to \, 5}$$

$$= 0.0906 - 0.0906$$

$$= 0.0000 \frac{m^3}{s}$$

Continuity equation is satisfied at the 4th node.
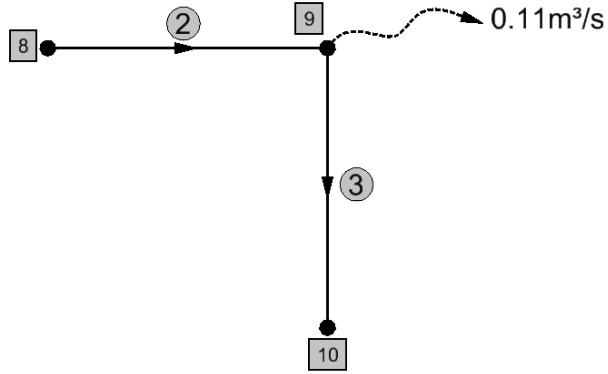

Figure A.12: Continuity for Node 5 in Test Case 3

Continuity equation for node 5 is as follows.

$$\sum Q_{inflow} = Q^{(2)}_{4 \, to \, 5} + Q^{(3)}_{4 \, to \, 5}$$

$$= 0.0467 + 0.0439$$

$$= 0.0906 \frac{m^3}{s}$$

$$\sum Q_{outflow} = Q^{(9)}_{5 \, to \, 7} + Q^{(8)}_{5 \, to \, 8}$$

$$= 0.0204 + 0.0701$$

$$= 0.0905 \frac{m^3}{s}$$

$$\sum Q_{inflow} - \sum Q_{outflow} = Q^{(2)}_{4 \, to \, 5} + Q^{(3)}_{4 \, to \, 5} - Q^{(9)}_{5 \, to \, 7} - Q^{(8)}_{5 \, to \, 8}$$

$$= 0.0906 - 0.0905$$

$$= 0.0001 \frac{m^3}{s}$$

Error is only $0.0001 m^3/s$. Continuity equation is satisfied at the 5th node.

Figure A.13: Continuity for Node 7 in Test Case 3

Continuity equation for node 7 is as follows.

$$\sum Q_{inflow} = Q^{(9)}_{5 \ to \ 7}$$
$$= 0.0204 \frac{m^3}{s}$$

$$\sum Q_{outflow} = Q^{(4)}_{7 \ to \ 6}$$
$$= 0.0204 \frac{m^3}{s}$$

$$\sum Q_{inflow} - \sum Q_{outflow} = Q^{(9)}_{5 \ to \ 7} - Q^{(4)}_{7 \ to \ 6}$$
$$= 0.0204 - 0.0204$$
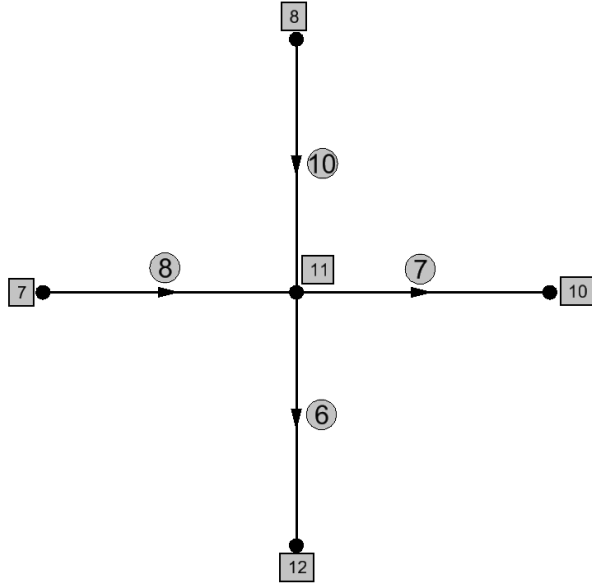$$= 0.0000 \frac{m^3}{s}$$

Continuity equation is satisfied at the 7th node.

Figure A.14: Continuity for Node 8 in Test Case 3

Continuity equation for node 8 is as follows.

$$\sum Q_{inflow} = Q^{(8)}_{5 \ to \ 8}$$

$$= 0.0701 \frac{m^3}{s}$$

$$\sum Q_{outflow} = Q^{(5)}_{8 \ to \ 9}$$

$$= 0.0701 \frac{m^3}{s}$$

$$\sum Q_{inflow} - \sum Q_{outflow} = Q^{(8)}_{5 \ to \ 8} - Q^{(5)}_{8 \ to \ 9}$$

$$= 0.0701 - 0.0701$$

$$= 0.0000 \frac{m^3}{s}$$

Continuity equation is satisfied at the 8th node.

A.4 Continuity Check for Each Node for Test Case 4
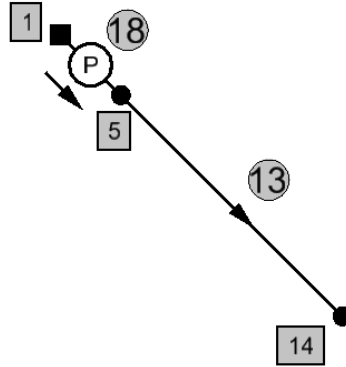
Figure A.15: Continuity for Node 5

Continuity equation for node 5 is as follows.

$$\sum Q_{inflow} = Q^{(18)}_{1 \ to \ 5}$$

$$= 0.5166 \frac{m^3}{s}$$

$$\sum Q_{outflow} = Q^{(13)}_{5 \text{ to } 14}$$

$$= 0.5166 \frac{m^3}{s}$$

$$\sum Q_{inflow} - \sum Q_{outflow} = Q^{(18)}_{1 \text{ to } 5} - Q^{(13)}_{5 \text{ to } 14}$$

$$= 0.5166 - 0.5166$$
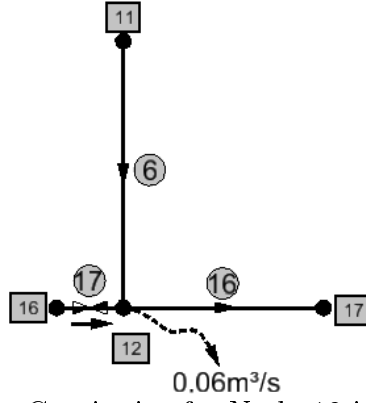
$$= 0.0000 \frac{m^3}{s}$$

Continuity equation is satisfied at the 5th node.

Figure A.16: Continuity for Node 6 in Test Case 4

Continuity equation for node 6 is as follows.

$$\sum Q_{inflow} = Q^{(5)}_{14 \text{ to } 6}$$

$$= 0.5166 \frac{m^3}{s}$$

$$\sum Q_{outflow} = Q^{(1)}_{6 \text{ to } 15} + Q^{(9)}_{6 \text{ to } 7}$$

$$= 0.2658 + 0.2658$$

$$= 0.5166 \frac{m^3}{s}$$

$$\sum Q_{inflow} - \sum Q_{outflow} = Q^{(5)}_{14 \text{ to } 6} - Q^{(1)}_{6 \text{ to } 15} - Q^{(9)}_{6 \text{ to } 7}$$

$$= 0.5166 - 0.2658 - 0.2658$$

$$= 0.0000 \frac{m^3}{s}$$
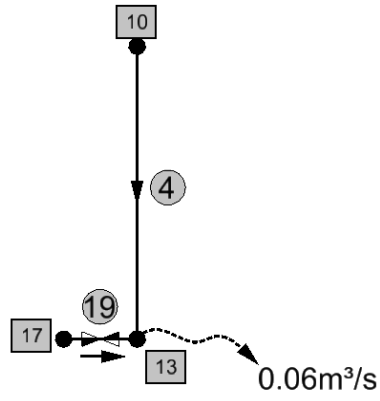
Continuity equation is satisfied at the 6th node.
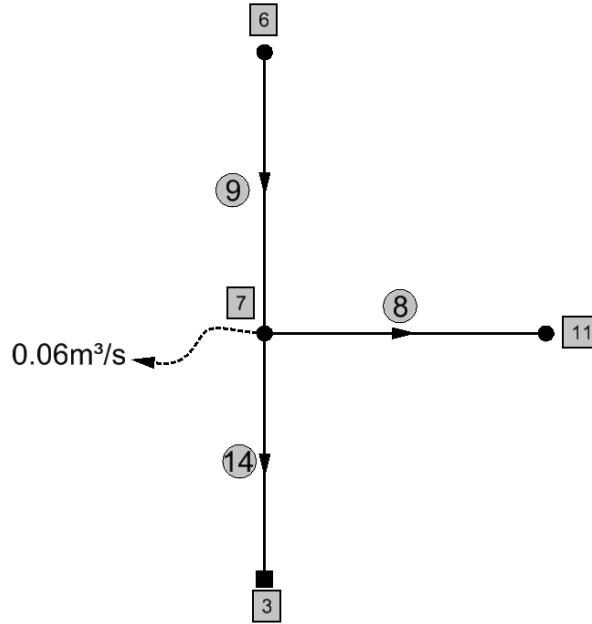
Figure A.17: Continuity for Node 7 in Test Case 4

Continuity equation for node 7 is as follows.

$$\sum Q_{inflow} = Q^{(9)}_{6 \ to \ 7}$$
$$= 0.2508 \frac{m^3}{s}$$

$$\sum Q_{outflow} = Q^{(14)}_{7 \ to \ 3} + Q^{(8)}_{7 \ to \ 11} + Q_7$$
$$= 0.0832 + 0.1077 + 0.0600$$
$$= 0.2509 \frac{m^3}{s}$$

$$\sum Q_{inflow} - \sum Q_{outflow} = Q^{(9)}_{6 \ to \ 7} - Q^{(14)}_{7 \ to \ 3} - Q^{(8)}_{7 \ to \ 11} - Q_7$$
$$= 0.2508 - 0.0832 - 0.1077 - 0.0600$$
$$= -0.0001 \frac{m^3}{s}$$

Error is only $0.0001 m^3/s$. Continuity equation is satisfied at the 7th node.

Figure A.18: Continuity for Node 8 in Test Case 4

Continuity equation for node 8 is as follows.

$$\sum Q_{inflow} = Q_{15\ to\ 8}^{(15)}$$
$$= 0.2658 \frac{m^3}{s}$$

$$\sum Q_{outflow} = Q_{8\ to\ 9}^{(2)} + Q_{8\ to\ 11}^{(10)}$$
$$= 0.1453 + 0.1205$$
$$= 0.2658 \frac{m^3}{s}$$

$$\sum Q_{inflow} - \sum Q_{outflow} = Q_{15\ to\ 8}^{(15)} - Q_{8\ to\ 9}^{(2)} - Q_{8\ to\ 11}^{(10)}$$
$$= 0.2658 - 0.1453 - 0.1205$$
$$= 0.0000 \frac{m^3}{s}$$
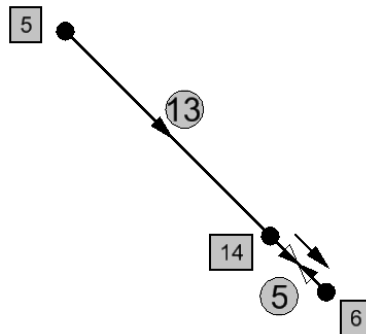
Continuity equation is satisfied at the 8th node.

94

Figure A.19: Continuity for Node 9 in Test Case 4

Continuity equation for node 9 is as follows.

$$\sum Q_{inflow} = Q^{(2)}_{8\ to\ 9}$$
$$= 0.1453 \frac{m^3}{s}$$

$$\sum Q_{outflow} = Q^{(3)}_{9\ to\ 10} + Q_9$$
$$= 0.0353 + 0.1100$$
$$= 0.1453 \frac{m^3}{s}$$

$$\sum Q_{inflow} - \sum Q_{outflow} = Q^{(2)}_{8\ to\ 9} - Q^{(3)}_{9\ to\ 10} - Q_9$$
$$= 0.1453 - 0.0353 - 0.1100$$
$$= 0.0000 \frac{m^3}{s}$$

Continuity equation is satisfied at the 9th node.

95
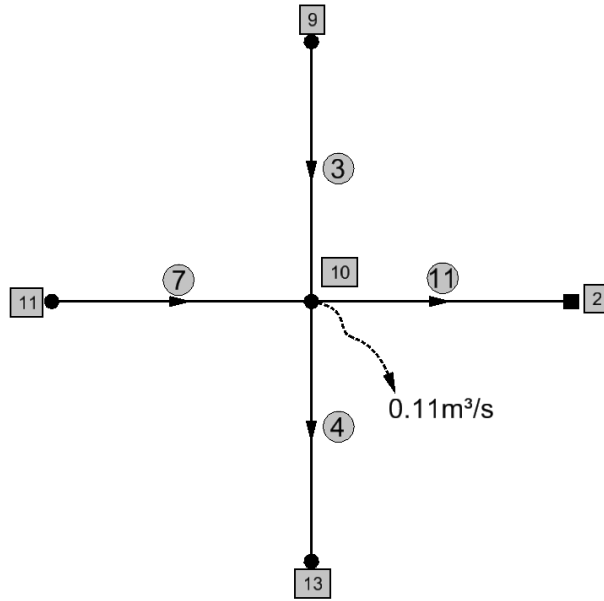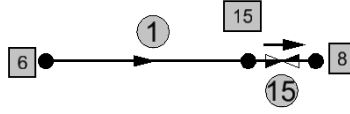
Figure A.20: Continuity for Node 10 in Test Case 4

Continuity equation for node 10 is as follows.

$$\sum Q_{inflow} = Q^{(7)}_{11 \ to \ 10} + Q^{(3)}_{9 \ to \ 10}$$
$$= 0.1357 + 0.0353$$
$$= 0.1710 \frac{m^3}{s}$$

$$\sum Q_{outflow} = Q^{(4)}_{10 \ to \ 13} + Q^{(11)}_{10 \ to \ 2} + Q_{10}$$
$$= 0.0563 + 0.0047 + 0.1100$$
$$= 0.1710 \frac{m^3}{s}$$

$$\sum Q_{inflow} - \sum Q_{outflow} = Q^{(7)}_{11 \ to \ 10} + Q^{(3)}_{9 \ to \ 10} - Q^{(4)}_{10 \ to \ 13} - Q^{(11)}_{10 \ to \ 2} - Q_{10}$$
$$= 0.1357 + 0.0353 - 0.0563 - 0.0047 - 0.1100$$
$$= 0.0000 \frac{m^3}{s}$$
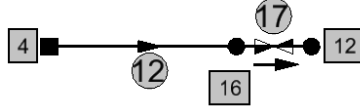
Continuity equation is satisfied at the 10th node.

96

Figure A.21: Continuity for Node 11 in Test Case 4

Continuity equation for node 11 is as follows.

$$\sum Q_{inflow} = Q^{(8)}_{7\ to\ 11} + Q^{(10)}_{8\ to\ 11}$$
$$= 0.1077 + 0.1205$$
$$= 0.2282 \frac{m^3}{s}$$

$$\sum Q_{outflow} = Q^{(7)}_{11\ to\ 10} + Q^{(6)}_{11\ to\ 12}$$
$$= 0.0925 + 0.1357$$
$$= 0.2282 \frac{m^3}{s}$$

$$\sum Q_{inflow} - \sum Q_{outflow} = Q^{(8)}_{7\ to\ 11} + Q^{(10)}_{8\ to\ 11} - Q^{(7)}_{11\ to\ 10} + Q^{(6)}_{11\ to\ 12}$$
$$= 0.1077 + 0.1205 - 0.0925 - 0.1357$$
$$= 0.0000 \frac{m^3}{s}$$

Continuity equation is satisfied at the 11th node.

97

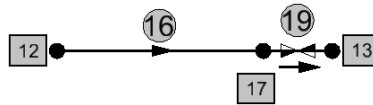Figure A.22:   Continuity for Node 12 in Test Case 4

Continuity equation for node 12 is as follows.

$$\sum Q_{inflow} = Q^{(17)}_{16 \ to \ 12} + Q^{(6)}_{11 \ to \ 12}$$
$$= 0.0228 + 0.0925$$
$$= 0.1153\frac{m^3}{s}$$

$$\sum Q_{outflow} = Q^{(16)}_{12 \ to \ 17} + Q_{12}$$
$$= 0.0553 + 0.0600$$
$$= 0.1153\frac{m^3}{s}$$

$$\sum Q_{inflow} - \sum Q_{outflow} = Q^{(17)}_{16 \ to \ 12} + Q^{(6)}_{11 \ to \ 12} - Q^{(16)}_{12 \ to \ 17} + Q_{12}$$
$$= 0.0228 + 0.0925 - 0.0553 - 0.0600$$
$$= 0.0000\frac{m^3}{s}$$
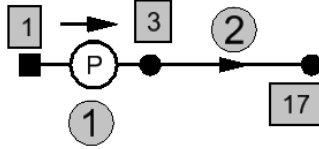
Continuity equation is satisfied at the 12th node.

Figure A.23: Continuity for Node 13 in Test Case 4

Continuity equation for node 13 is as follows.

$$\sum Q_{inflow} = Q^{(19)}_{17\ to\ 13} + Q^{(4)}_{10\ to\ 13}$$
$$= 0.0553 + 0.0047$$
$$= 0.0600 \frac{m^3}{s}$$

$$\sum Q_{outflow} = Q_{13}$$
$$= 0.0600 \frac{m^3}{s}$$

$$\sum Q_{inflow} - \sum Q_{outflow} = Q^{(19)}_{17\ to\ 13} + Q^{(4)}_{10\ to\ 13} - Q_{13}$$
$$= 0.0553 + 0.0047 - 0.0600$$
$$= 0.0000 \frac{m^3}{s}$$
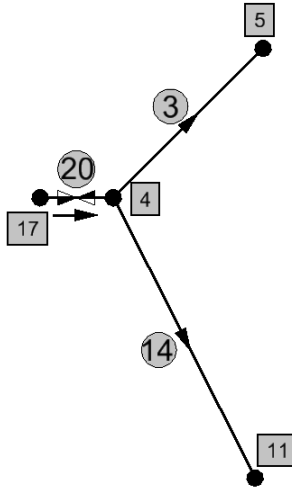
Continuity equation is satisfied at the 13th node.

Figure A.24: Continuity for Node 14 in Test Case 4

Continuity equation for node 14 is as follows.

$$\sum Q_{inflow} = Q^{(13)}_{5\ to\ 14}$$

$$= 0.5166 \frac{m^3}{s}$$

$$\sum Q_{outflow} = Q^{(5)}_{14\ to\ 6}$$

$$= 0.5166 \frac{m^3}{s}$$

$$\sum Q_{inflow} - \sum Q_{outflow} = Q^{(13)}_{5\ to\ 14} - Q^{(5)}_{14\ to\ 6}$$

$$= 0.5166 - 0.5166$$

$$= 0.0000 \frac{m^3}{s}$$

Continuity equation is satisfied at the 14th node.

Figure A.25:   Continuity for Node 15 in Test Case 4

Continuity equation for node 15 is as follows.

$$\sum Q_{inflow} = Q^{(1)}_{6\ to\ 15}$$

$$= 0.2658 \frac{m^3}{s}$$

$$\sum Q_{outflow} = Q^{(15)}_{15\ to\ 8}$$

$$= 0.2658 \frac{m^3}{s}$$

$$\sum Q_{inflow} - \sum Q_{outflow} = Q^{(1)}_{6\ to\ 15} - Q^{(15)}_{15\ to\ 8}$$

$$= 0.2658 - 0.2658$$

$$= 0.0000 \frac{m^3}{s}$$

Continuity equation is satisfied at the 15th node.

Figure A.26: Continuity for Node 16 in Test Case 4

Continuity equation for node 16 is as follows.

$$\sum Q_{inflow} = Q^{(12)}_{4\ to\ 16}$$
$$= 0.0228\frac{m^3}{s}$$

$$\sum Q_{outflow} = Q^{(17)}_{16\ to\ 12}$$
$$= 0.0228\frac{m^3}{s}$$

$$\sum Q_{inflow} - \sum Q_{outflow} = Q^{(12)}_{4\ to\ 16} - Q^{(17)}_{16\ to\ 12}$$
$$= 0.0228 - 0.0228$$
$$= 0.0000\frac{m^3}{s}$$

Continuity equation is satisfied at the 16th node.

Figure A.27: Continuity for Node 17 in Test Case 4

Continuity equation for node 17 is as follows.

$$\sum Q_{inflow} = Q^{(16)}_{12\ to\ 17}$$
$$= 0.0553\frac{m^3}{s}$$

$$\sum Q_{outflow} = Q_{17 \ to \ 13}^{(19)}$$

$$= 0.0553 \frac{m^3}{s}$$

$$\sum Q_{inflow} - \sum Q_{outflow} = Q_{12 \ to \ 17}^{(16)} - Q_{17 \ to \ 13}^{(19)}$$

$$= 0.0553 - 0.0553$$

$$= 0.0000 \frac{m^3}{s}$$

Continuity equation is satisfied at the 17th node.

A.5   Continuity Check for Each Node for Test Case 5

Figure A.28:   Continuity for Node 3 in Test Case 5

Continuity equation for node 3 is as follows.

$$\sum Q_{inflow} = Q_{1 \ to \ 3}^{(1)}$$

$$= 0.8233 \frac{m^3}{s}$$

$$\sum Q_{outflow} = Q_{3 \ to \ 17}^{(2)}$$

$$= 0.8233 \frac{m^3}{s}$$

$$\sum Q_{inflow} - \sum Q_{outflow} = Q_{1 \ to \ 3}^{(1)} - Q_{3 \ to \ 17}^{(2)}$$

$$= 0.8233 - 0.8233$$

$$= 0.0000 \frac{m^3}{s}$$

Continuity equation is satisfied at the 3rd node.
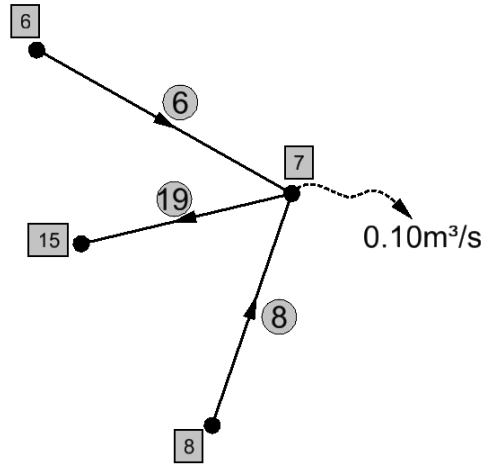
Figure A.29: Continuity for Node 4 in Test Case 5

Continuity equation for node 4 is as follows.

$$\sum Q_{inflow} = Q^{(20)}_{17 \ to \ 4}$$
$$= 0.8233 \frac{m^3}{s}$$

$$\sum Q_{outflow} = Q^{(3)}_{4 \ to \ 5} + Q^{(14)}_{4 \ to \ 11}$$
$$= 0.4591 + 0.3643$$
$$= 0.8234 \frac{m^3}{s}$$

$$\sum Q_{inflow} - \sum Q_{outflow} = Q^{(20)}_{17 \ to \ 4} - Q^{(3)}_{4 \ to \ 5} - Q^{(14)}_{4 \ to \ 11}$$
$$= 0.8232 - 0.4591 - 0.3643$$
$$= -0.0001 \frac{m^3}{s}$$

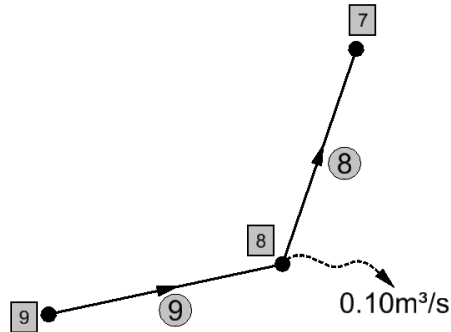Error is only $0.0001 m^3/s$. Continuity equation is satisfied at the 4th node.
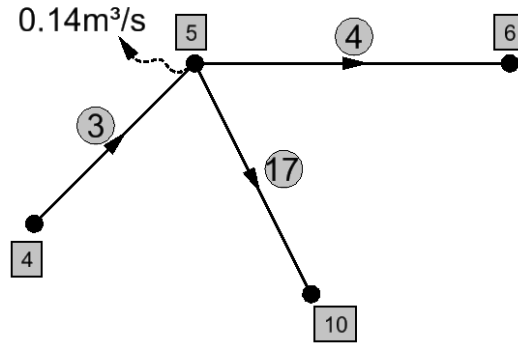
Figure A.30: Continuity for Node 5 in Test Case 5

Continuity equation for node 5 is as follows.

$$\sum Q_{inflow} = Q^{(3)}_{4 \ to \ 5}$$
$$= 0.4591 \frac{m^3}{s}$$

$$\sum Q_{outflow} = Q^{(4)}_{5 \ to \ 6} + Q^{(17)}_{5 \ to \ 10} + Q_5$$
$$= 0.1733 + 0.1457 + 0.1400$$
$$= 0.4590 \frac{m^3}{s}$$

$$\sum Q_{inflow} - \sum Q_{outflow} = Q^{(3)}_{4 \ to \ 5} - Q^{(4)}_{5 \ to \ 6} - Q^{(17)}_{5 \ to \ 10} - Q_5$$
$$= 0.4591 - 0.1733 - 0.1457 - 0.1400$$
$$= 0.0001 \frac{m^3}{s}$$

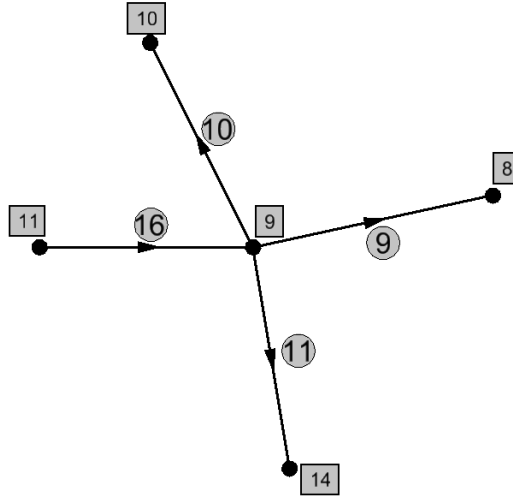Error is only $0.0001^{m^3}/_s$. Continuity equation is satisfied at the 5th node.
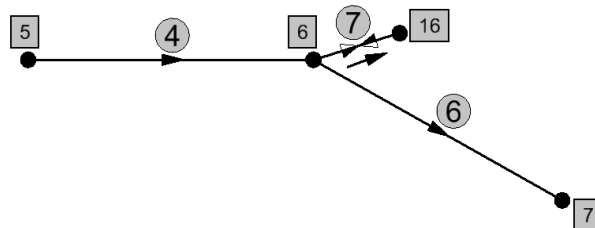
Figure A.31: Continuity for Node 6 in Test Case 5

Continuity equation for node 6 is as follows.

$$\sum Q_{inflow} = Q^{(4)}_{5\ to\ 6}$$

$$= 0.1733 \frac{m^3}{s}$$

$$\sum Q_{outflow} = Q^{(7)}_{6\ to\ 16} + Q^{(7)}_{6\ to\ 7}$$

$$= 0.0933 + 0.0800$$

$$= 0.1733 \frac{m^3}{s}$$

$$\sum Q_{inflow} - \sum Q_{outflow} = Q^{(4)}_{5\ to\ 6} - Q^{(7)}_{6\ to\ 16} - Q^{(7)}_{6\ to\ 7}$$

$$= 0.1733 - 0.0933 - 0.0800$$

$$= 0.000 \frac{m^3}{s}$$

Continuity equation is satisfied at the 6th node.

Figure A.32: Continuity for Node 7 in Test Case 5

Continuity equation for node 7 is as follows.

$$\sum Q_{inflow} = Q^{(6)}_{6\ to\ 7} + Q^{(8)}_{8\ to\ 7}$$

$$= 0.0800 + 0.0243$$

$$= 0.1043 \frac{m^3}{s}$$

$$\sum Q_{outflow} = Q^{(7)}_{7 \; to \; 15} + Q_7$$

$$= 0.0043 + 0.1000$$

$$= 0.1043\frac{m^3}{s}$$

$$\sum Q_{inflow} - \sum Q_{outflow} = Q^{(6)}_{6 \; to \; 7} + Q^{(8)}_{8 \; to \; 7} - Q^{(7)}_{7 \; to \; 15} - Q_7$$

$$= 0.0800 + 0.0243 - 0.0043 - 0.1000$$

$$= 0.0000\frac{m^3}{s}$$

Continuity equation is satisfied at the 7th node.

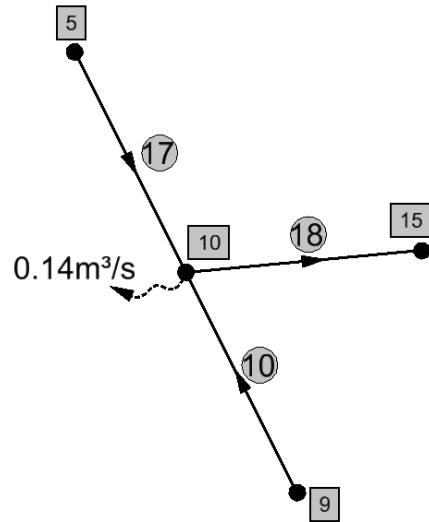
Figure A.33:   Continuity for Node 8 in Test Case 5

Continuity equation for node 8 is as follows.

$$\sum Q_{inflow} = Q^{(9)}_{9 \; to \; 8}$$

$$= 0.1243\frac{m^3}{s}$$

$$\sum Q_{outflow} = Q^{(8)}_{8 \; to \; 7} + Q_8$$

$$= 0.0243 + 0.1000$$

$$= 0.1243\frac{m^3}{s}$$

$$\sum Q_{inflow} - \sum Q_{outflow} = Q^{(9)}_{9 \; to \; 8} - Q^{(8)}_{8 \; to \; 7} - Q_8$$

$$= 0.1243 - 0.0243 - 0.1000$$
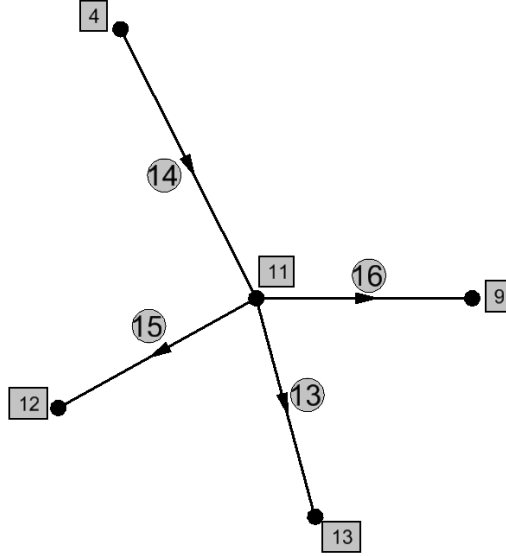
$$= 0.0000\frac{m^3}{s}$$

Continuity equation is satisfied at the 8th node.

Figure A.34: Continuity for Node 9 in Test Case 5

Continuity equation for node 9 is as follows.

$$\sum Q_{inflow} = Q^{(16)}_{11 \; to \; 9}$$
$$= 0.2384 \frac{m^3}{s}$$

$$\sum Q_{outflow} = Q^{(10)}_{9 \; to \; 10} + Q^{(9)}_{9 \; to \; 8} + Q^{(11)}_{9 \; to \; 14}$$
$$= 0.0749 + 0.1243 + 0.0391$$
$$= 0.2383 \frac{m^3}{s}$$

$$\sum Q_{inflow} - \sum Q_{outflow} = Q^{(16)}_{11 \; to \; 9} - Q^{(10)}_{9 \; to \; 10} - Q^{(9)}_{9 \; to \; 8} - Q^{(11)}_{9 \; to \; 14}$$
$$= 0.2384 - 0.0749 - 0.1243 - 0.0391$$
$$= 0.0001 \frac{m^3}{s}$$

Error is only $0.0001 m^3/s$. Continuity equation is satisfied at the 9th node.
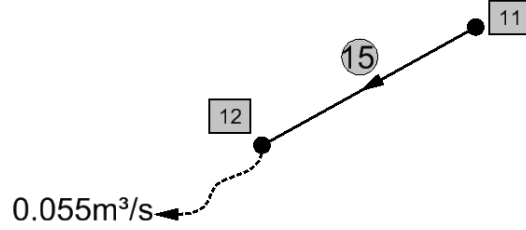
Figure A.35: Continuity for Node 10 in Test Case 5

Continuity equation for node 10 is as follows.

$$\sum Q_{inflow} = Q_{5\ to\ 10}^{(17)} + Q_{9\ to\ 10}^{(10)}$$
$$= 0.1457 + 0.0749$$
$$= 0.2206 \frac{m^3}{s}$$

$$\sum Q_{outflow} = Q_{10\ to\ 15}^{(18)} + Q_{10}$$
$$= 0.0.0807 + 0.1400$$
$$= 0.2207 \frac{m^3}{s}$$

$$\sum Q_{inflow} - \sum Q_{outflow} = Q_{5\ to\ 10}^{(17)} + Q_{9\ to\ 10}^{(10)} - Q_{10\ to\ 15}^{(18)} - Q_{10}$$
$$= 0.1457 + 0.0749 - 0.0807 - 0.1400$$
$$= -0.0001 \frac{m^3}{s}$$

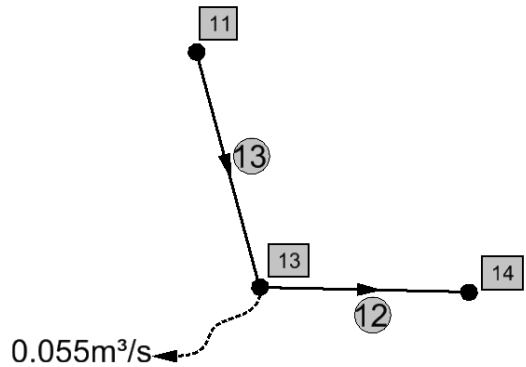Error is only $0.0001 m^3/s$. Continuity equation is satisfied at the 10th node.

Figure A.36: Continuity for Node 11 in Test Case 5

Continuity equation for node 11 is as follows.

$$\sum Q_{inflow} = Q^{(14)}_{4 \; to \; 11}$$
$$= 0.3643 \frac{m^3}{s}$$

$$\sum Q_{outflow} = Q^{(16)}_{11 \; to \; 9} + Q^{(13)}_{11 \; to \; 13} + Q^{(15)}_{11 \; to \; 12}$$
$$= 0.2384 + 0.0709 + 0.0550$$
$$= 0.3643 \frac{m^3}{s}$$

$$\sum Q_{inflow} - \sum Q_{outflow} = Q^{(14)}_{4 \; to \; 11} - Q^{(16)}_{11 \; to \; 9} - Q^{(13)}_{11 \; to \; 13} - Q^{(15)}_{11 \; to \; 12}$$
$$= 0.3643 - 0.2384 - 0.0709 - 0.0550$$
$$= 0.0000 \frac{m^3}{s}$$

Continuity equation is satisfied at the 11th node.

Figure A.37: Continuity for Node 12 in Test Case 5

Continuity equation for node 12 is as follows.

$$\sum Q_{inflow} = Q^{(15)}_{11\ to\ 12}$$
$$= 0.0550\frac{m^3}{s}$$

$$\sum Q_{outflow} = Q_{12}$$
$$= 0.0550\frac{m^3}{s}$$

$$\sum Q_{inflow} - \sum Q_{outflow} = Q^{(15)}_{11\ to\ 12} - Q_{12}$$
$$= 0.0550 - 0.0550$$
$$= 0.0000\frac{m^3}{s}$$

Continuity equation is satisfied at the 12th node.
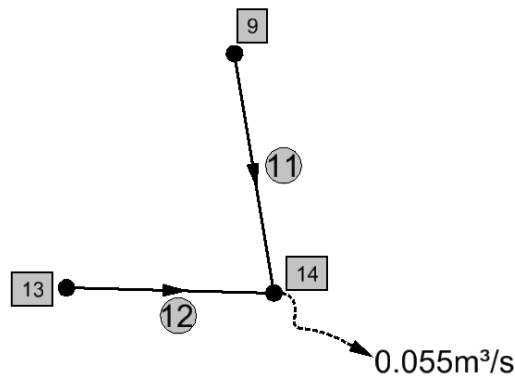

Figure A.38: Continuity for Node 13 in Test Case 5

Continuity equation for node 13 is as follows.

110

$$\sum Q_{inflow} = Q^{(13)}_{11\ to\ 13}$$

$$= 0.0709 \frac{m^3}{s}$$

$$\sum Q_{outflow} = Q^{(12)}_{13\ to\ 14} + Q_{13}$$

$$= 0.0159 + 0.0550$$

$$= 0.0708 \frac{m^3}{s}$$

$$\sum Q_{inflow} - \sum Q_{outflow} = Q^{(13)}_{11\ to\ 13} - Q^{(12)}_{13\ to\ 14} - Q_{13}$$

$$= 0.0709 - 0.0159 - 0.0550$$

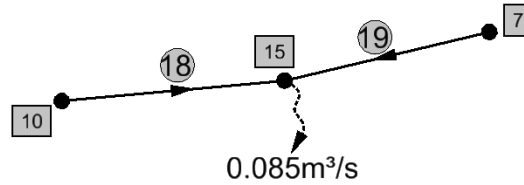$$= 0.0000 \frac{m^3}{s}$$

Continuity equation is satisfied at the 13th node.

Figure A.39: Continuity for Node 14 in Test Case 5

Continuity equation for node 14 is as follows.

$$\sum Q_{inflow} = Q^{(11)}_{9\ to\ 14} + Q^{(12)}_{13\ to\ 14}$$

$$= 0.0391 + 0.0159$$

$$= 0.0550 \frac{m^3}{s}$$

$$\sum Q_{outflow} = Q_{14}$$

$$= 0.0550 \frac{m^3}{s}$$

$$\sum Q_{inflow} - \sum Q_{outflow} = Q^{(11)}_{9 \; to \; 14} + Q^{(12)}_{13 \; to \; 14} - Q_{14}$$

$$= 0.0391 + 0.0159 - 0.0550$$

$$= 0.0000 \frac{m^3}{s}$$

Continuity equation is satisfied at the 14th node.

Figure A.40:   Continuity for Node 15 in Test Case 5

Continuity equation for node 15 is as follows.

$$\sum Q_{inflow} = Q^{(18)}_{10 \; to \; 15} + Q^{(19)}_{7 \; to \; 15}$$

$$= 0.0807 + 0.0043$$

$$= 0.0850 \frac{m^3}{s}$$

$$\sum Q_{outflow} = Q_{15}$$

$$= 0.0850 \frac{m^3}{s}$$

$$\sum Q_{inflow} - \sum Q_{outflow} = Q^{(18)}_{10 \; to \; 15} + Q^{(19)}_{7 \; to \; 15} - Q_{15}$$

$$= 0.0807 + 0.0043 - 0.0850$$

$$= 0.0000 \frac{m^3}{s}$$
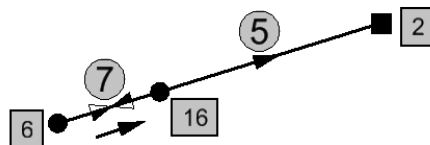
Continuity equation is satisfied at the 15th node.

Figure A.41:   Continuity for Node 16 in Test Case 5

Continuity equation for node 16 is as follows.

$$\sum Q_{inflow} = Q^{(7)}_{6 \ to \ 16}$$

$$= 0.0933 \frac{m^3}{s}$$

$$\sum Q_{outflow} = Q^{(5)}_{16 \ to \ 2}$$

$$= 0.0933 \frac{m^3}{s}$$

$$\sum Q_{inflow} - \sum Q_{outflow} = Q^{(7)}_{6 \ to \ 16} - Q^{(5)}_{16 \ to \ 2}$$

$$= 0.0933 - 0.0933$$

$$= 0.0000 \frac{m^3}{s}$$
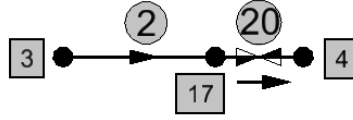
Continuity equation is satisfied at the 16th node.

Figure A.42: Continuity for Node 17 in Test Case 5

Continuity equation for node 17 is as follows.

$$\sum Q_{inflow} = Q^{(2)}_{3 \ to \ 17}$$

$$= 0.8233 \frac{m^3}{s}$$

$$\sum Q_{outflow} = Q^{(20)}_{17 \ to \ 4}$$

$$= 0.8233 \frac{m^3}{s}$$

$$\sum Q_{inflow} - \sum Q_{outflow} = Q^{(2)}_{3 \ to \ 17} - Q^{(20)}_{17 \ to \ 4}$$

$$= 0.8233 - 0.8233$$

$$= 0.0000 \frac{m^3}{s}$$

Continuity equation is satisfied at the 17th node.

113